Boron isotope compositions establish the origin of marble from metamorphic complexes: Québec, New York, and Sri Lanka

CORINNE KUEBLER[1,*,†], ANTONIO SIMONETTI[1], STEFANIE S. SIMONETTI[1], AND ROBERT F. MARTIN[2]

[1]Department of Civil and Environmental Engineering and Earth Sciences, University of Notre Dame, Notre Dame, Indiana 46556, U.S.A.
[2]Earth & Planetary Sciences, McGill University, 3450 University Street, Montreal, Québec H3A 0E8, Canada

ABSTRACT

The origin of an array of marble samples found in both the Grenville Province and southwestern Sri Lanka remains uncertain, whether magmatic, sedimentary, or mixed, due to their proximity to both carbonatite bodies and carbonate-rich metasedimentary rocks. This study reports boron and trace element abundances, in addition to carbon, oxygen, boron, and strontium isotopic compositions, to determine the petrogenesis of these carbonate-rich samples. Boron abundances for all of the samples are relatively high and variable (1.48–71.1 ppm) compared to those for carbonatites worldwide ($\leq$1 ppm), and mostly overlap those documented for sedimentary sources (up to 54 ppm). The rare earth element (REE) abundances (0.5–1068 ppm) for the marbles studied are similar to those for local sedimentary units and thus contain, in general, lower REE contents than both the average worldwide calcio-carbonatite and respective neighboring carbonatite bodies. The $\delta^{13}C_{V\text{-}PDB}$ and $\delta^{18}O_{V\text{-}SMOW}$ compositions for all of the samples range between –2.9 to +3.2 ± 0.1‰ and +14.3 to +25.8 ± 0.2‰, respectively, and are considerably heavier than those reported for magmatic or metamorphosed carbonatites. The $^{87}Sr/^{86}Sr$ ratios reported here range from 0.70417 to 0.70672, which are more radiogenic than the average $^{87}Sr/^{86}Sr$ (~0.70345) reported for carbonatites included for comparison in this study. Importantly, the boron isotopic compositions ($\delta^{11}B$‰) for samples from the Grenville Province range from +7.5 to +15.7 ± 0.5‰, which are consistent with those reported for biogenic carbonate (+4.9 to +35.1‰). In contrast, $\delta^{11}B$ values for the samples of marble from Sri Lanka vary from –9.8 to –14.3 ± 0.5‰ overlapping with those estimated for average bulk continental crust (–9.1 ± 2.4‰). Together, the boron compositions, chemical data, stable (C, O), and radiogenic Sr isotopic data overwhelmingly point to a sedimentary origin for the marble samples examined here. Specifically, the samples from the Grenville Province represent marble formed during high-temperature regional metamorphism of limestone units. The Sri Lankan samples were formed from carbonate-rich and ^{11}B-poor fluids derived from a crustal source. The boron isotopic compositions for the samples studied here are also compared to those reported for mantle-derived carbonate (i.e., carbonatites) worldwide, along with their associated $\delta^{13}C_{V\text{-}PDB}$ and $^{87}Sr/^{86}Sr$ values. This comparison results in defining three isotopically distinct fields; mantle-derived carbonates, sedimentary carbonates derived from heterogeneous limestone protoliths, and carbonates derived from meteoric water interacting with crustal material. This work establishes the effective use of boron isotopic compositions in determining the origin of carbonate-rich rocks of contentious petrogenesis.

Keywords: Boron isotopes, Grenville Province, Sri Lanka, multi-colored marble, carbonatite; Lithium, Beryllium, and Boron: Quintessentially Crustal

INTRODUCTION

Deciphering the petrogenesis of carbonate-rich rocks in crustal regimes, whether igneous (carbonatite), sedimentary (limestone), or metamorphic (marble), in some instances can be difficult, especially as there are multiple possible modes of formation. Because of their similarities in both appearance and major-element compositions, several criteria have been used to distinguish carbonatites (of igneous affinity) from metasedimentary carbonate rocks; these include field relationships (e.g., the occurrence of fenites; Barker 1989), distinctive mineral assemblages (e.g., the presence of pyrochlore; Hogarth

1989; Le Bas et al. 2002), trace and rare earth element (REE) concentrations, chondrite-normalized REE patterns (Le Bas et al. 2002), and stable isotope compositions (e.g., Gittins et al. 1970; Deines 1989). These lines of evidence can be combined to argue for a sedimentary or igneous origin, but are not without exceptions. The debate would benefit from additional geochemical signatures.

One such example of carbonate-rich rocks with unclear origin(s) is found within the Grenville Province in southern Ontario and adjacent Québec (Canada), and extending into the proximal Adirondack region of New York State (U.S.A.). Commonly referred to as marbles (the term adopted here), skarns, carbonatites, vein-dikes, or pseudo-carbonatites, these rocks can be found scattered throughout the Central Metasedimentary Belt (CMB) and its boundary zones (Fig. 1). Previous work on these

* E-mail: ckuebler@nd.edu. Orcid 0000-0002-2779-4184
† Special collection papers can be found online at http://www.minsocam.org/MSA/ AmMin/special-collections.html.

15
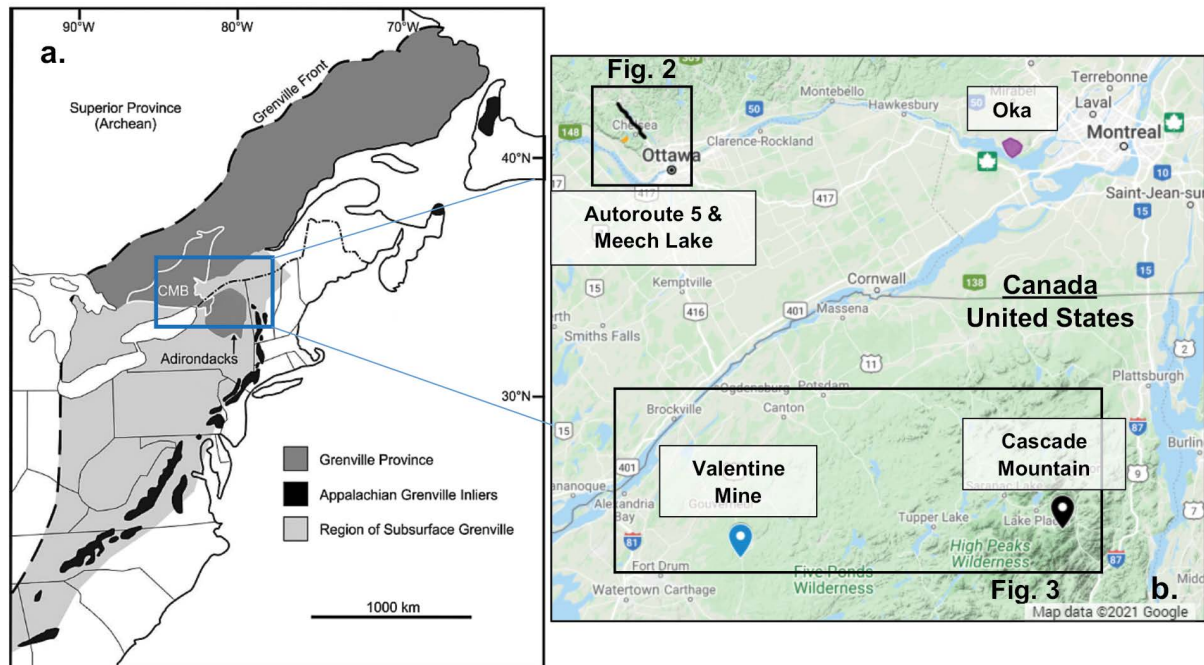
Figure 1. (**a**) Simplified map of the Grenville Province modified from Matt et al. (2017) after Tollo et al. (2010). Central Metasedimentary Belt (CMB) is outlined in white. (**b**) Sample location map within Canada (black line; along Autoroute 5) and New York (BC-Harris-Valentine Mine, BC-Cascade-Cascade Mountain) from Google Maps. Also shown are the Oka (purple field, main map) and Meech Lake (orange field within Fig. 2 box) carbonatite complexes. See Figures 2 and 3 for more details. (Color online.)

marbles have focused on traditional geochemical signatures (Sr, Nd, C, O isotopic ratios, REE geochemistry, major and trace element concentrations) in addition to field relationships and mineralogy (Adams and Barlow 1910; Satterly 1956; Hewitt 1967; Gittins et al. 1970; Valley and O'Neil 1984; Lentz 1996; Moecher et al. 1997; Chiarenzelli et al. 2019). Several models describing their formation, including those with an igneous, sedimentary, or mixed origin, have been proposed for these marbles, and these are: (1) contact metamorphism and an influx of regional fluids from surrounding metasediments (Kitchen and Valley 1995; Bailey et al. 2019); (2) localized interaction between limestone and an intrusive body that released fluids forming a skarn-type deposit (Gerdes and Valley 1994; Chiarenzelli et al. 2019); (3) melting and remobilization of pre-existing carbonate deposit(s) (Moyd 1990; Lentz 1999; Sinaei-Esfahani 2013; Schumann and Martin 2016; Schumann et al. 2019); (4) metamorphosed carbonatite (Moecher et al. 1997); and (5) coeval formation with magmatic carbonate from nearby carbonatites (i.e., Meech Lake or Oka carbonatite complexes; Lumbers et al. 1990). Given the various models for their formation and their location, a new constraint on the petrogenesis of these marbles may provide additional insights into the complicated tectono-magmatic history of the Grenville Province and Adirondacks (Gerdes and Valley 1994; Moecher et al. 1997).

An analogous geological situation is present in Sri Lanka, where multi-colored, calcite-rich marble (term also adopted here), skarn, or dike-like units occur with an unclear genesis, whether derived from remobilized marble or carbonatite-related fluids (Madugalla et al. 2014; Madugalla and Pitawala 2015; Pitawala

2019). Previous work on these carbonate units in Sri Lanka have mainly focused on the economic viability of these deposits (i.e., lime and carbonate-derived products; Mantilaka et al. 2013, 2014a, 2014b); however, a few studies contain information on their geochemical characteristics (e.g., mineralogy, stable isotopic signatures, and trace element abundances; Madugalla et al. 2014; Madugalla and Pitawala 2015; Pitawala 2019). Pitawala (2019) suggested that their formation is due to marble remobilization as a result of shearing related to the assembly of Gondwana. To provide new insights into the provenance and formation model of the carbonate units in both the Grenville Province and Sri Lanka, this study investigates a suite of multi-colored carbonate-rich rocks from these regions through the lens of a new forensic tool based on boron abundances and corresponding isotope compositions.

BORON AS A KEY GEOCHEMICAL INDICATOR

Boron-related investigations of geological samples are advantageous for many reasons, including its use as a paleo-pH proxy in marine carbonates (e.g., Deegan et al. 2016; Rasbury and Hemming 2017; Rae 2018), isotopic sensitivity, especially in fluid-mediated processes (e.g., Spivack and Edmond 1987; Lemarchand et al. 2000, 2002; Gaillardet and Lemarchand 2018; De Hoog and Savov 2018), and limited isotopic fractionation during high-temperature metamorphism and/or hydrothermal activity associated with mantle-derived carbonates (e.g., Çimen et al. 2018, 2019; Kuebler et al. 2020). Boron is a widespread trace element in natural carbonates (~1 to 100 ppm; Kowalski and Wunder 2018 and references therein); its incorporation depends on the conditions of the precipitating fluid (e.g., pH,

temperature), the presence of other elements (e.g., Mg, Sr), and the type of carbonate present (biogenic or inorganic; Hemming and Hanson 1992; Hemming et al. 1995; Sanyal et al. 2000; Penman et al. 2013; Rasbury and Hemming 2017; Sutton et al. 2018). Although the mechanism(s) of B incorporation into the carbonate structure is complex, the most straightforward substitution is considered to be the exchange of the carbonate ion (CO_3^{2-}) with the borate ion (HBO_3^{2-}) due to the similarity in size (B-O and C-O bonds; 1.28 vs. 1.36 Å), charge, and shape (trigonal; Hemming and Hanson 1992; Hemming et al. 1995; Balan et al. 2016; Branson 2018). Importantly, boron isotopes (^{10}B and ^{11}B) are characterized by a high-mass difference (~10%), which leads to significant isotopic variation (~100‰; Palmer and Swihart 1996; Foster et al. 2016). In addition, because B is incompatible in the mantle- and partial-melting-related processes, B concentrations are <1 ppm and isotopically light ($\delta^{11}B = -7.1 \pm 0.9‰$) in the asthenospheric (MORB-like) mantle (Marschall et al. 2017). Conversely, sedimentary sources are characterized by an increase in both boron abundances (>> 1 ppm) and ^{11}B ($\delta^{11}B$ up to +35.1‰; Vengosh et al. 1991; Ishikawa and Nakamura 1993; Sutton et al. 2018). In recent studies, boron has proven to be a powerful diagnostic tool even in complicated geologic settings. For instance, it has been possible to elucidate the mantle source region(s) of the Miaoya and Bayan Obo carbonatite complexes in China despite extensive hydrothermal activity or high-grade metamorphism or both (Çimen et al. 2018, 2019; Kuebler et al. 2020). Furthermore, combining boron isotope values with C, O, and Sr isotope compositions has established an effective means for identifying pristine (unaltered) mantle-derived carbonate samples that can then be used to decipher the chemical nature of their upper mantle source regions (Hulett et al. 2016; Çimen et al. 2018, 2019; Kuebler et al. 2020).

Given the distinct boron signatures within various terrestrial reservoirs and its isotopic sensitivity as a tracer in fluid-related processes, the boron isotope compositions for samples of marble from the Grenville Province and Sri Lanka are used in this study to help delineate their origin. While several previous studies have examined the boron compositions of other minerals (e.g., tourmaline, serendibite, harkerite) within the Grenville Province (Grew et al. 1990, 1991, 1999; Belley et al. 2014), to our knowledge this is the first to examine the boron compositions of the carbonate within the Grenville Province and Sri Lanka marble units. Thus, this study will significantly contribute to understanding the nature of the fluids involved with their formation. A comparison of the results obtained here for the multi-colored calcite-rich samples from the Grenville Province and Sri Lanka with analogous data from worldwide carbonatites further reinforces the effectiveness of boron compositions in identifying magmatic vs. sedimentary carbonate, and the occurrence of any crustal contamination (if igneous in origin).

GEOLOGICAL BACKGROUND AND SAMPLE DESCRIPTIONS

Grenville Province and the Adirondacks

There are several geologic units related to the 15 samples of marble examined in this study from the northeastern region of North America, herein referred to as the Grenville Province samples (Fig. 1), that are discussed below with sample locations and geologic context shown in Figures 2 and 3. In summary,

the Grenville Province is a tectonically complicated region composed of overlapping accreted terranes that experienced extensive regional metamorphism with estimated temperatures up to 700–750 °C and pressures of 7–8 kilobars (Valley and O'Neil 1984; Kretz 2001) during the Grenville orogeny (~1.35 to 1.0 Ga; e.g., Valley and O'Neil 1984; Kretz 2001; Dickin and McNutt 2007 and references therein). The Adirondacks are part of the Grenville Province located near the foreland region of the Appalachian Orogeny (Fig. 3; Chiarenzelli et al. 2018). They are subdivided into two regions, the Highlands and Lowlands, based on lithology and metamorphic grade (Fig. 3). The Highlands consist of granulite-facies meta-igneous and -sedimentary rocks that were deformed during two major orogenic events (~1165 Ma, Shawinigan Orogeny and ~1050 Ma, Ottawan Orogeny; McLelland et al. 2013; Chiarenzelli and Selleck 2016). In contrast, the Lowlands are characterized by amphibolite-grade metamorphic facies assemblages that consist of supracrustal rocks of the Grenville Supergroup that were metamorphosed during the Shawinigan Orogeny (Chiarenzelli et al. 2015).

Two carbonatite complexes intruding the Grenville Province (Figs. 1 and 2) are relevant to this study; Oka and Meech Lake. The ~120 million-year-old Oka carbonatite complex (OCC; Chen and Simonetti 2013) is located ~94 km east of the sample locality in Canada (Autoroute 5) and ~150 km north of the New York samples. The OCC consists of both carbonatite and undersaturated silicate rocks (e.g., ijolite, alnöite) in a distorted figure eight that intrudes a Precambrian host gneiss and is surrounded by fenite (e.g., Chen and Simonetti 2013). The Meech Lake carbonatite complex (MLCC) is about ~4 km from the main area of sample collection in Canada and consists of numerous carbonatite dikes that cut a Mesoproterozoic aplitic granite plug within the Wakefield orthogneiss batholith, in small, discontinuous, and concentric fractures (Fig. 2 overlay; Vistelius et al. 1983; Hogarth 2016).

All of the Grenville Province marble samples examined here are hosted in part of the Grenville Supergroup (Baillieul 1976; Gerdes and Valley 1994; Chamberlain et al. 1999; Bailey et al. 2019; Chiarenzelli et al. 2019). These marbles are characterized by their abundance of large, well-formed minerals in crystal "pockets" due to the local dissolution of the calcite matrix (Chiarenzelli et al. 2019). More specifically, 13 samples of marble were collected from exposures along Autoroute 5, in the 2.5 km interval between Farm Point and Wakefield (Fig. 2; see field guide, Belley et al. 2016). The Wakefield area is situated within the southeastern corner of the Marble Domain, Mont-Laurier Terrane, where marbles have been metamorphosed to upper amphibolite–granulite facies conditions (Cartwright and Weaver 1993; Corriveau 2013). The outcrops along Autoroute 5 are different from the regional marble (white to gray) due to the variety of colors present (i.e., white, blue, green, orange, yellow); however, these pockets of colored marble exist in other parts of the Grenville Province as well (Kretz 2001). The petrography and mineralogy of these deposits are discussed in detail in Sinaei-Esfahani (2013), Schumann and Martin (2016), and Belley et al. (2016). The samples studied here are of six different colors: various shades of blue (WAK-087, WAK-02, BCJF, BC-ST4), yellow (YC-01–YC-03), orange (OC-ST1, OC-ST3), green (GC-01), white/cream (WCJF, PC-01), and gray (JF). All of the
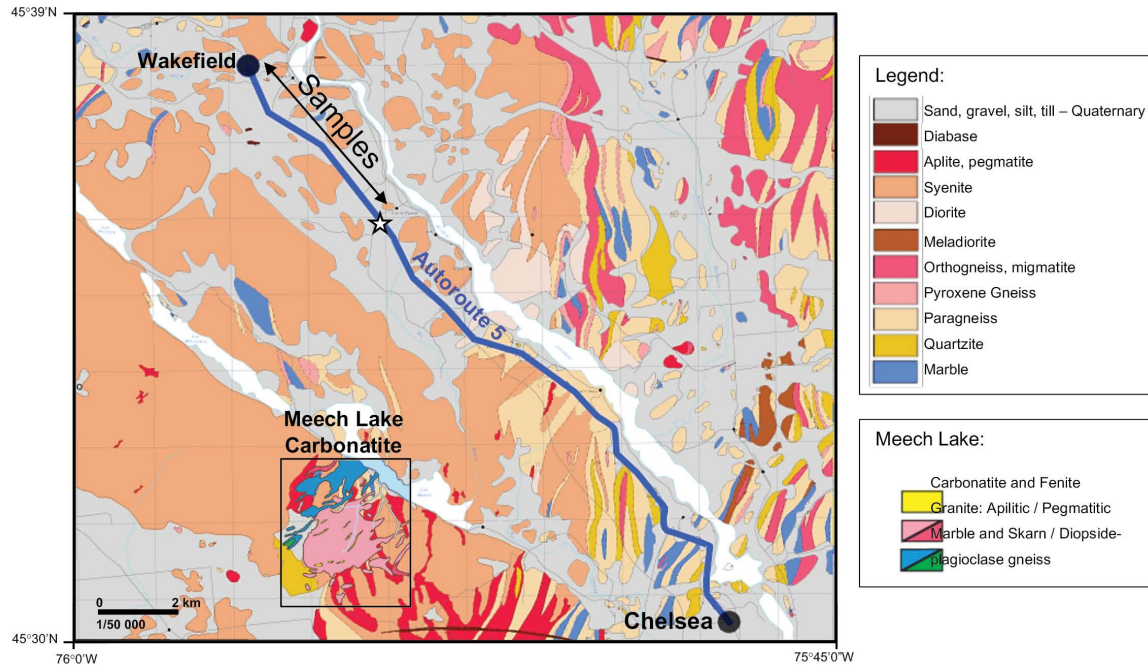
FIGURE 2. Geologic map of the Autoroute 5 (blue line) area from Wakefield to Chelsea in Québec, Canada (modified after Béland 1955). Samples from this area were taken from outcrops along the route (between Wakefield and the white star). A more detailed geologic map of the Meech Lake carbonatite complex is outlined in black (after Hogarth 2016). (Color online.)
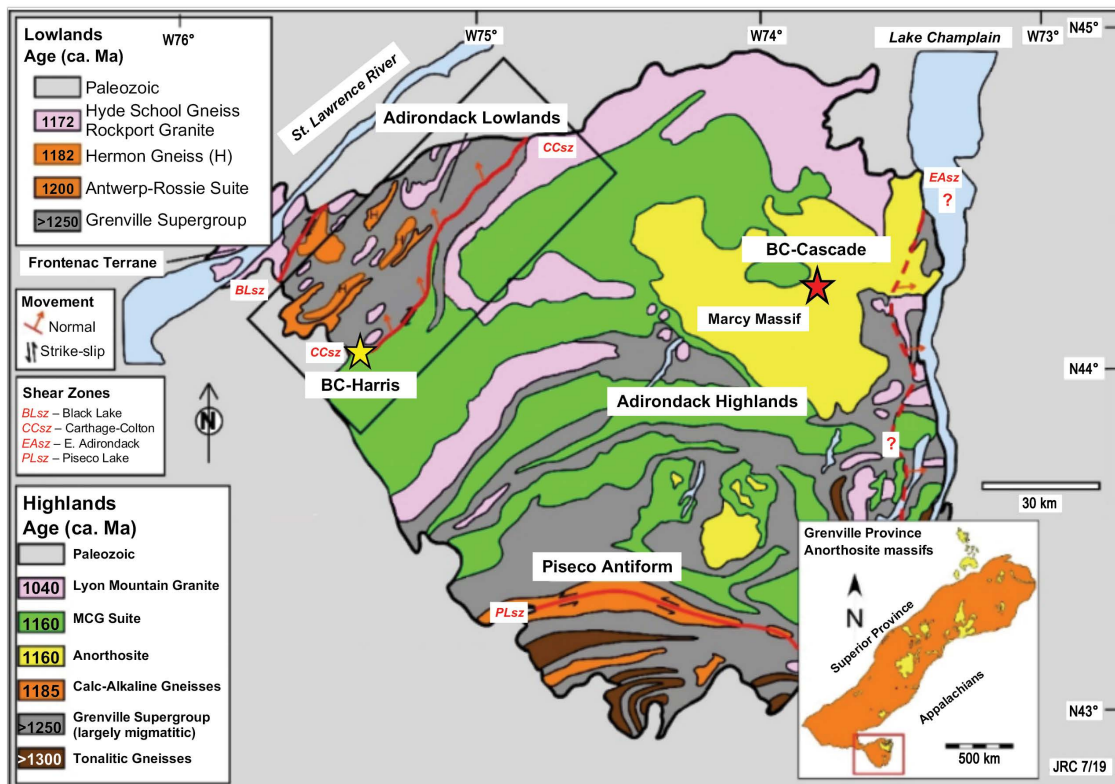
FIGURE 3. Detailed geologic map of the Adirondack Lowlands and Highlands after Chiarenzelli et al. (2019). The inset shows the contiguous Grenville Province (orange). The two samples of marble taken from this region are indicated with stars (yellow, BC-Harris; red, BC-Cascade). (Color online.)

samples range in size from 1 to 4 cm (Fig. 4).

The two blue marble samples obtained from the Adirondacks (Fig. 3) were retrieved from the Valentine mine, near Harrisville, New York (BC-Harris) and the Cascade Slide, the northern slope of Cascade Mountain, Keene, New York (BC-Cascade). The BC-Harris sample was collected from a "sky-blue" marble near a wollastonite skarn that grades into white marble further away (Gerdes and Valley 1994; Chamberlain et al. 1999). The marble surrounds the skarn and is also in contact with the Diana syenite complex that was emplaced at 1.15 Ga (Gerdes and Valley 1994; Chamberlain et al. 1999; Basu and Premo 2001). The BC-Cascade sample was collected near a wollastonite-garnet granulite within the Marcy Anorthosite Massif, which is believed to represent post-metamorphic (~1.15 Ga) domal uplift (Baillieul 1976; Kitchen and Valley 1995).

Sri Lanka

The basement geology of Sri Lanka consists of high-grade Precambrian metamorphic rocks, which are subdivided into four lithotectonic units based on metamorphic grade, Nd-model ages, and structural features (Kröner et al. 1991; Cooray 1984, 1994); these four units are the Highland Complex (HC), the Wanni Complex (WC), the Vijayan Complex (VC), and the Kadugannawa Complex (KC) as shown in Figure 5. The HC,

the most extensive unit, is composed of metasedimentary rocks (e.g., quartzite, marble, pelitic to semi-pelitic gneiss), and late- to post-tectonic granitoids and mafic magmatic rocks (Cooray 1994; Fernando et al. 2017) that yield Nd-model ages of 3.4–2.0 Ga (Milisenda et al. 1988, 1994). The WC consists of a suite of gneisses and granites with metasediments mostly occurring near the border with the HC (Cooray 1994; Kröner et al. 2003) that yield Nd model ages ranging from 1.0–2.0 Ga (Milisenda et al. 1988, 1994). Both HC and WC experienced upper amphibolite to granulite-facies metamorphism (Cooray 1994) from 600 to 550 Ma (Milisenda et al. 1994). The boundary between the WC and HC is still poorly defined (e.g., Fig. 5; Kröner et al. 2003). The KC sits at the center of the island and is dominated by hornblende-bearing gneisses with Nd model ages of 2.0–1.0 Ga (Milisenda et al. 1988, 1994), whereas the VC at the south of Sri Lanka is mainly composed of amphibolite facies gneisses and metasediments with Nd model ages of 1.8–1.1 Ga (Milisenda et al. 1988, 1994). The thrust fault boundary between VC and HC has been postulated to be a result of the final assembly of Gondwana (He et al. 2016).

Also indicated in Figure 5 is the location of the Eppawala carbonatite (EC), the main carbonatite unit in Sri Lanka, which crops out within the WC (Manthilake et al. 2008; Madugalla et al. 2017). The EC consists of apatite-rich carbonate rocks that occur

FIGURE 4. Images of selected samples examined in this study. Each yellow bar indicates 1 cm. (Color online.)
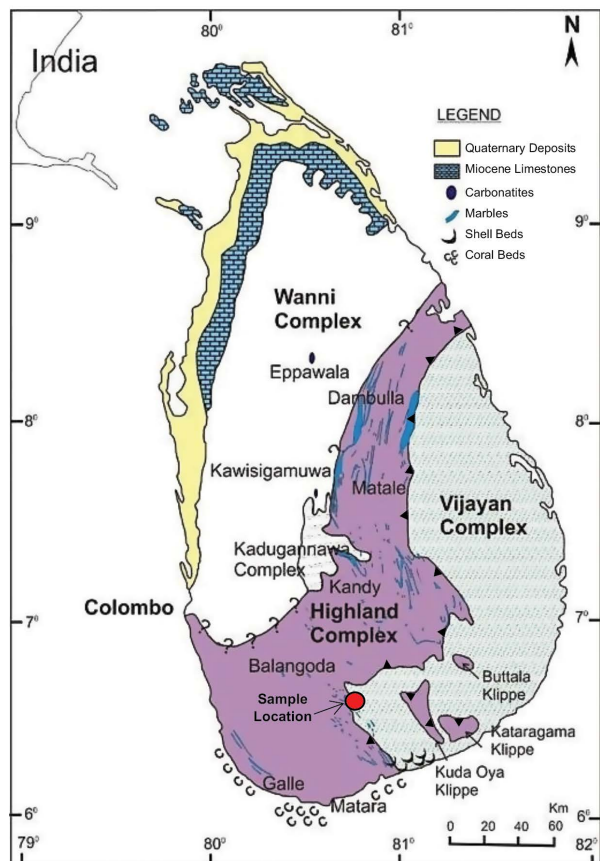
Figure 5. Simplified geologic map of Sri Lanka showing occurrences of marbles, carbonatites, limestones and other carbonate rocks from Pitawala (2019) after Cooray (1984). Sample locality is identified with the red circle. (Color online.)

as massive, discontinuous N-S-trending oval bodies and intrude the Precambrian, high-grade metamorphic terrane (WC) close to the village of Eppawala, north of the city of Kandy (Pitawala et al. 2003; Madugalla et al. 2017). Based on field evidence and Rb-Sr and Sm-Nd isotopic data, the EC was emplaced within the WC after a period of high-grade metamorphism that occurred at ~550 Ma (Weerakoon et al. 2001); this relates the emplacement of the EC to large-scale regional faulting of the Indian subcontinent associated with carbonatite intrusions in south India (Viladkar and Subramanian 1995; Pitawala and Lottermoser 2012).

Of importance to this study are the widely distributed marbles throughout the HC (shown in Fig. 5), especially those near the VC boundary (sample locality). Overall, the marbles occur as layers or intercalations (10–20 km along strike) with pelitic gneiss and mafic granulites that have been deformed, metamorphosed, and recrystallized under granulite facies *P-T* conditions, thus obscuring primary sedimentary features (Cooray 1984; Osanai et al. 2000, 2006; Pitawala 2019). The marble layers in the SW region of Sri Lanka trend northwesterly and have gneissose banding with both silicate-rich and pure marble layers (Pitawala 2019). The samples of colored marble examined in this study were collected from the Piyangiriya quarry (06°36.054′ N, 80°50.261′ E), which is located south of the city of Kandy and near the border

between the HC and VC units (Fig. 5). In this area, dike-like calcitic carbonate bodies (2–20 m wide; 20–150 m long) transect marble, pelitic gneiss, and charnockitic gneiss (Madugalla et al. 2014; Madugalla and Pitawala 2015) as blue to yellow-brown lenticular marble bodies (Pitawala 2019). Two samples in this study (SL-01 and SL-10) are blue and sample SL-07 is yellow; specimens range in size from 1 to 2.5 cm (Fig. 4).

ANALYTICAL METHODS

Boron and trace element abundances

Samples of marble were crushed, then carbonate fractions were hand-picked with the aid of a binocular microscope and powdered by mortar and pestle. These carbonate separates were processed for determinations of boron and trace element abundances in a class 1000 clean-room laboratory at the Midwest Isotope and Trace Element Research Analytical Center (MITERAC), University of Notre Dame. Detailed analytical procedures and instrumental protocols are included within the Online Materials[1].

Stable (C, O, B) and radiogenic (Sr) isotope analyses

Carbon and oxygen isotope analyses were conducted in the Center for Environmental Science and Technology (CEST) at the University of Notre Dame using a Delta V Advantage isotope ratio mass spectrometer. Further details on the analytical procedure are contained within the Online Materials[1]. Both B and Sr isotope analyses were conducted in MITERAC via solution-mode on a Nu PlasmaII multi-collector-ICP-MS (MC-ICP-MS). Detailed ion exchange chemistry and instrumental setup for B and Sr isotopic ratio determinations can also be found within the Online Materials[1].

To evaluate the potential effects of weathering, leaching experiments were conducted using small fragments (0.3–0.7 mm) of samples soaked in 0.5 mL of 2% HNO_3 at room temperature for ~18 h. The leachate was removed, and the residual solid was dried at 65 °C then completely dissolved in high-purity 16 N HNO_3 acid. Both leachate and residual aliquots were processed through the B-specific ion-exchange chemistry and analyzed on the MC-ICP-MS following the procedures described in the Online Materials[1].

RESULTS

Trace element geochemistry

The boron and trace element abundances for the marble samples are reported in Table 1. The boron contents range from 1.48 to 71.1 ppm, which overlap documented B concentrations for various carbonate sediments (0.3–26 ppm; Ishikawa and Nakamura 1993; Spivack and You 1997; Vengosh et al. 1991) and biogenic carbonate (e.g., foraminifera, 9–54 ppm; Vengosh et al. 1991). These concentrations are also higher than the ≤1 ppm B reported for the vast majority of carbonatites worldwide (Hulett et al. 2016; Çimen et al. 2018, 2019; Kuebler et al. 2020). The total rare earth element (REE) contents for the samples vary from 0.5 to 1068 ppm (Table 1). Most of the corresponding chondrite-normalized (CN)-REE patterns (Fig. 6) show light rare earth element (LREE) enrichment (La/Lu$_{(CN)}$ = 2.8–1491), with the exception of sample OC-ST3 from the Grenville Province (orange line; Fig. 6a; La/Lu$_{(CN)}$ = 0.7).

The majority of the Grenville Province samples have much lower total REE contents than the average calcio-carbonatite worldwide (Woolley and Kempe 1989) and Meech Lake carbonatite (Fig. 6a; Hogarth 2016), with the exception of three samples (OC-ST1, OC-ST3, PC-01), which have higher heavy REE abundances (HREE; Er to Lu). The majority of the Grenville Province samples have CN-REE patterns similar to the Otter Lake regional (white) marble, a representative sample of regional marble (76 km NW of Autoroute 5; Sinaei-Esfahani 2013), and have concentra-

tions that are intermediate between the marble sampled at Otter Lake and the Oka carbonatite field (Chen and Simonetti 2015). The Adirondack samples are highlighted in Figure 6a, which displays the distinct steeply sloped CN-REE pattern for sample BC-Cascade (green line). Figure 6c is a CN-REE plot that highlights the patterns for several of the samples taken along Autoroute 5, and these are compared to that for the Otter Lake marble (dashed pink line).

The Sri Lanka marble samples also have much lower total REE contents than the average calcio-carbonatite (Woolley and Kempe 1989) and the Eppawala carbonatite (Manthilake et al. 2008; Pitawala et al. 2003), with the exception of the La content for sample SL-07 (200 ppm; Table 1). As Figure 6b shows, sample SL-07 has overlapping Ce-Sm contents with the carbonatite dikes, but mid-to-heavy REE abundances that are intermediate between values reported for carbonatite dikes and regional marbles (Pitawala 2019). In contrast, samples SL-01 and SL-10 have lower La-Eu contents than the Sri Lankan regional marbles with comparable Gd-Lu concentrations. The CN-REE pattern for SL-07 is similar to the carbonatite dike field, whereas samples SL-01 and SL-10 have patterns more akin to the regional marble field (Fig. 6b).

Boron, carbon, and oxygen isotope compositions

Carbon (C) and oxygen (O) isotopic ratios for the samples examined here are listed in Table 2 and are compared to corresponding data for proximal geologic units within their respective areas (Fig. 7). The carbon and oxygen isotope compositions for

TABLE 2. Carbon, oxygen, and boron isotopic data for samples of multi-colored marble

	$\delta^{13}C_{V-PDB}$ (‰)	Uncertainty (2σ)	$\delta^{18}O_{V-SMOW}$ (‰)	Uncertainty (2σ)	$\delta^{11}B^a$ (‰)
SL-01	−1.2	0.1	18.7	0.2	−14.3
SL-07	−0.5	0.1	19.4	0.1	−9.8
SL-10	−0.4	0.1	20.0	0.1	−10.5
BC-Harris	1.8	0.1	25.0	0.1	10.8
BC-Cascade	−1.0	0.1	21.5	0.1	7.5
WAK-02	−2.5	0.1	18.4	0.1	9.7
WAK-07	−2.9	0.1	17.4	0.1	11.2
BCJF	2.6	0.1	25.4	0.1	10.2
BC-ST4	3.0	0.1	25.8	0.1	12.5
WCJF	1.6	0.1	22.8	0.1	8.3
GC-01	2.3	0.1	25.4	0.1	14.6
YC-01	3.2	0.1	21.9	0.1	10.7
YC-02	3.2	0.1	21.5	0.1	15.7
YC-03	2.9	0.1	25.7	0.1	11.4
OC-ST1	−0.8	0.1	14.5	0.1	13.0
OC-ST3	−0.9	0.1	17.5	0.1	14.1
PC-01	−0.8	0.1	14.3	0.1	7.8
JF	3.0	0.1	23.9	0.1	13.3

^{a} $\delta^{11}B$ associated 2σ uncertainty (±0.5‰) based on replicate analyses of in-house coral standard.

the marble samples range between −2.9‰ to +3.2‰ and +14.3‰ to +25.8‰, respectively, and are significantly heavier than those reported for magmatic carbonatites ($\delta^{13}C_{V-PDB} \sim -4$‰ to −8‰ and $\delta^{18}O_{V-SMOW} \sim +6$‰ to +10‰; Keller and Hoefs 1995; Fig. 7). In addition, the carbon and oxygen isotopic values for all of the samples fall outside the range attributed to metamorphosed carbonatites (Moecher et al. 1997). The Grenville Province samples have significantly heavier carbon and oxygen isotopic

TABLE 1. Trace element abundances (parts per million) for marble samples in this study

	SL-01	SL-07	SL-10	BC-Harris	BC-Cascade	Wak-02	Wak-07	Bcjf	BC-ST4	Wcjf	GC-01	YC-01	YC-02	YC-03	OC-ST1	OC-ST3	Pc-01	JF
Color	b	y	b	b	b	b	b	b	b	w	gr	y	y	y	o	o	c	g
B	1.53	2.44	1.48	6.43	71.1	25.4	4.93	8.98	8.30	7.13	12.8	2.53	2.77	3.49	11.4	4.38	8.14	14.3
Li	0.0	0.0	0.0	0.0	0.0	0.0	0.0	0.2	0.0	0.3	0.1	0.2	0.4	0.1	0.1	0.3	0.5	0.5
Sc	0.1	0.1	0.1	0.0	0.0	0.0	0.0	0.2	0.1	0.3	0.1	0.1	0.1	0.1	0.4	0.1	0.2	0.1
Co	0.2	0.5	0.1	0.0	0.1	0.1	0.1	0.1	0.2	0.1	0.2	0.1	0.1	0.1	0.2	0.2	0.1	0.1
Ni	5.3	5.6	3.9	1.4	1.3	3.8	3.7	3.0	2.9	2.3	3.6	3.2	3.1	2.8	2.9	3.1	2.0	2.9
Cu	0.6	0.3	0.2	0.1	0.1	0.3	0.6	0.4	0.5	0.2	0.2	0.2	0.1	0.3	0.9	0.2	4.1	1.3
Zn	0.8	3.1	0.5	bdl	4.2	bdl	4.1	1.8	3.0	0.8	1.6	3.1	3.8	4.5	7.7	1.5	11.2	5.4
Rb	0.0	0.0	0.1	0.0	0.0	0.1	0.0	0.2	0.0	0.1	0.0	0.1	0.1	0.1	0.0	0.4	0.3	0.1
Sr	146	1035	85	4942	633	2985	3237	417	238	643	612	757	705	2819	6842	1565	4459	1416
Y	1.4	16.2	0.6	4.2	0.2	9.4	4.9	1.4	2.2	5.5	21.6	4.2	4.9	10.7	294	153	82.3	14.1
Zr	0.1	0.2	0.0	0.0	0.0	0.2	0.1	0.0	0.0	0.0	0.2	0.2	0.2	0.1	4.6	0.0	0.0	0.1
Nb	0.1	0.0	0.0	0.0	0.0	0.0	0.0	0.0	0.0	0.0	0.0	0.1	0.1	0.0	3.1	0.0	0.0	0.0
Mo	0.0	0.3	0.0	0.1	0.0	0.0	0.2	0.0	0.0	bdl	0.1	0.0	0.0	0.0	0.3	0.0	0.2	0.1
Cs	0.0	0.0	0.1	0.0	0.0	0.0	0.0	0.0	0.0	0.0	0.0	0.0	0.0	0.0	0.0	0.0	0.0	0.0
Ba	12.9	181	9.4	262	24.5	29.2	1032	15.8	1239	16.1	204	99.1	86.7	3127	311	14.3	8774	54.2
La	0.3	200	0.1	4.7	18.9	32.5	26.5	0.9	1.6	56.4	40.0	37.4	30.0	94.7	338	12.0	142	56.1
Ce	0.3	25.5	0.2	2.5	116	20.1	11.1	1.8	1.6	76.3	26.1	27.3	29.3	32.3	393	38.9	224	79.3
Pr	0.1	2.0	0.0	0.3	7.8	1.6	1.0	0.2	0.2	5.6	2.9	2.6	2.6	2.7	40.2	6.5	24.6	8.1
Nd	0.1	5.5	0.0	1.1	22.7	5.2	3.1	0.7	1.1	16.4	10.2	7.2	7.4	7.9	165	37.4	115	26.6
Sm	0.0	0.6	0.0	0.2	1.5	0.7	0.4	0.2	0.2	1.7	1.5	0.7	0.7	0.7	24.7	10.5	19.1	3.1
Eu	0.0	0.1	0.0	0.0	0.2	0.1	0.1	0.1	0.1	0.5	0.3	0.1	0.2	0.2	5.2	2.1	4.4	0.7
Gd	0.0	0.4	0.0	0.2	0.9	0.6	0.3	0.2	0.3	1.2	1.4	0.6	0.7	0.6	21.4	12.4	16.0	2.2
Tb	0.0	0.0	0.0	0.0	0.1	0.1	0.0	0.0	0.0	0.1	0.2	0.1	0.1	0.1	3.1	2.0	2.3	0.3
Dy	0.1	0.2	0.0	0.2	0.2	0.5	0.2	0.2	0.2	0.6	1.1	0.4	0.5	0.3	19.6	13.0	13.8	1.3
Ho	0.0	0.0	0.0	0.0	0.0	0.1	0.0	0.0	0.1	0.1	0.3	0.1	0.1	0.1	5.4	3.2	3.6	0.3
Er	0.0	0.1	0.0	0.1	0.0	0.4	0.1	0.1	0.1	0.3	0.6	0.2	0.3	0.2	17.9	9.4	11.0	0.7
Tm	0.0	0.0	0.0	0.0	0.0	0.1	0.0	0.0	0.0	0.0	0.1	0.0	0.0	0.0	3.3	1.4	1.9	0.1
Yb	0.0	0.1	0.0	0.1	0.0	0.4	0.1	0.1	0.1	0.2	0.6	0.2	0.4	0.1	27.4	10.3	16.1	0.7
Lu	0.0	0.0	0.0	0.0	0.0	0.1	0.0	0.0	0.0	0.0	0.1	0.0	0.1	0.0	4.7	1.7	2.8	0.1
W	0.0	0.0	bdl	0.0	0.0	0.1	0.0	0.0	0.1	0.0	bdl	0.0	0.0	0.0	0.2	0.1	0.6	0.0
Pb	0.3	6.6	0.9	5.2	1.4	1.5	1.4	4.2	2.5	11.3	12.5	31.5	33.7	11.3	14.2	2.6	4.0	18.3
Th	0.0	3.0	0.1	0.3	0.3	0.0	0.5	0.2	0.1	0.0	0.8	2.6	0.8	0.2	0.2	0.8	0.0	1.5
U	0.1	0.3	0.3	0.1	1.3	0.2	0.3	0.0	0.0	0.1	0.1	0.2	0.1	0.0	14.5	0.0	0.1	0.1
TREEs	1.0	234	0.5	9.4	168	62.5	42.8	4.5	5.7	159	85.4	76.9	72.3	140	1068	161	597	180

Notes: bdl = below detection limit; TREEs = Total of all rare earth element abundances; color notation = blue (b), yellow (y), white (w), green (gr), orange (o), cream (c), gray (g); ICP-MS-determined elemental abundances, which are associated with relative uncertainties of between 3 to 5% (2σ level); Sri Lankan samples = SL-01, SL-07, SL-10; Grenville Province samples = BC-Harris, BC-Cascade, WAK-02, WAK-07, BCJF, BC-ST4, WCJF, GC-01, YC-01, YC-02, YC-03, OC-ST1, OC-ST3, PC-01, JF.
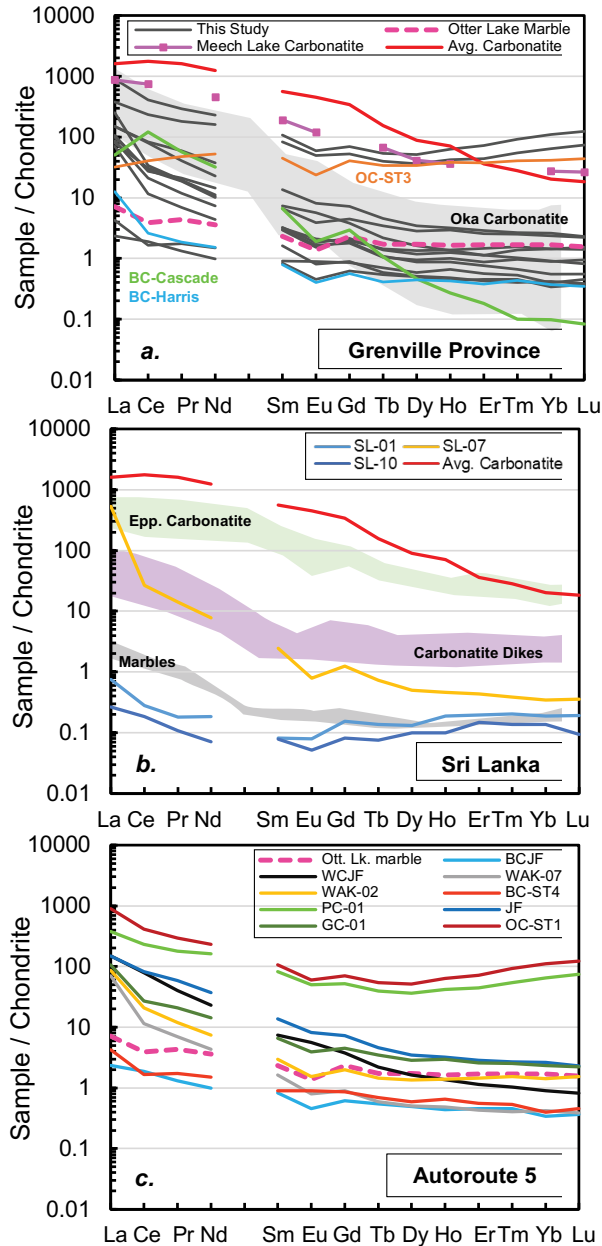
FIGURE 6. Chondrite-normalized (CN) REE patterns for samples analyzed in this study. (**a**) Samples of marble from the Grenville Province are compared to: Meech Lake carbonatite (purple; Hogarth 2016); Oka carbonatite (gray shaded field; Chen and Simonetti 2015); and a regional marble from Otter Lake, Québec (pink dashed line; Sinaei-Esfahani 2013). Several samples have been highlighted (orange = OC-ST3; blue = BC-Cascade; green = BC-Harris; see text for details). (**b**) Samples of multi-colored marble from Sri Lanka are compared to several local carbonate-rich rocks (shaded regions): Eppawala carbonatite (green; Manthilake et al. 2008; Pitawala et al. 2003); Carbonatite dikes (purple; Pitawala 2019); Marbles (gray; Pitawala 2019). The color of the CN-REE patterns for marble samples analyzed in **b** are based on their respective color in hand specimen. Also plotted in **a** and **b** is the average calcio-carbonatite (red line) from Woolley and Kempe (1989). (**c**) Samples from the Autoroute 5 locality compared to Otter Lake marble (pink dashed line; Sinaei-Esfahani 2013). Chondrite data are from Sun and McDonough (1989). (Color online.)

values compared to data reported for the Oka carbonatite complex (Chen and Simonetti 2015). Instead, they mostly overlap with the Lowlands Marble field (Kitchen and Valley 1995), with several falling within or just outside the range of C and O isotope compositions for skarns and marbles from the Central Metasedimentary Belt (CMB; Lentz 1999). Noteworthily, the Sri Lanka samples have C vs. O isotope signatures that plot between those for the Eppawala carbonatite and nearby metasedimentary units (Fig. 7b) and within the field defined by Sri Lankan carbonate-rich dikes (Pitawala 2019).

The boron isotopic ratios obtained for the samples investigated here are listed in Table 2. A comparison of the $\delta^{11}B$ values vs. the corresponding strontium isotopic ratios for the Grenville Province samples is shown in Figure 8b. The boron isotopic values for all samples of marble examined here are plotted against their corresponding $\delta^{13}C_{V-PDB}$ and Sr isotopic ratios in Figures 9b and 9c, respectively, along with those for carbonatites worldwide
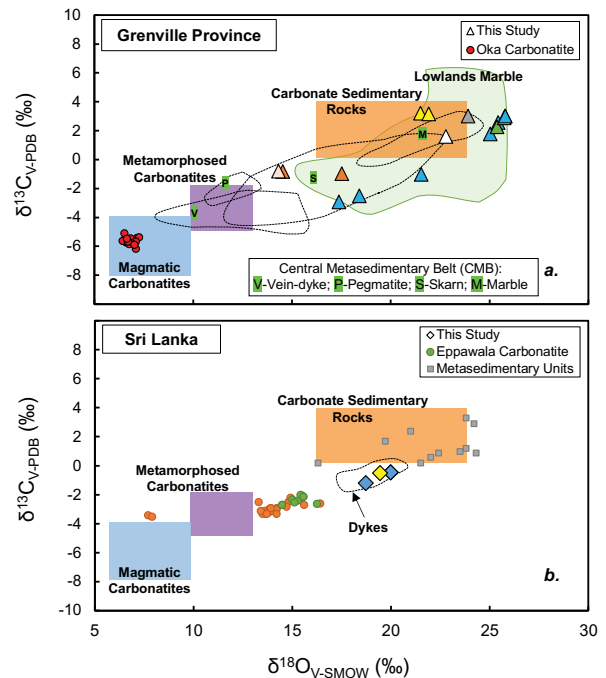
FIGURE 7. $\delta^{13}C_{V-PDB}$ (‰) vs. $\delta^{18}O_{V-SMOW}$ (‰) values for marble samples examined in this study. The shaded areas indicate fields for magmatic (blue) and metamorphosed (purple) carbonatites, in addition to carbonate sedimentary rocks (orange), from Chiarenzelli et al. (2019). The color of each sample (this study) is reflected in each individual symbol [(**a**) triangles; (**b**) diamonds]. (**a**) Isotope data for samples of multi-colored marble from Grenville Province are compared to those for the Oka carbonatite (red circles; Chen and Simonetti 2015), Lowlands marble (green shaded area; Kitchen and Valley 1995), and different parts of the Central Metasedimentary Belt (CMB; black dotted outlines; after Lentz 1999). (**b**) Isotope compositions for Sri Lanka samples are compared to those for metasedimentary units (gray squares: Pitawala et al. 2003) and the Eppawala carbonatite (orange circles: Pitawala et al. 2003; green circles: Manthilake et al. 2008). Also plotted (black dotted field) is the range of C vs. O isotopic compositions for Sri Lankan carbonate-rich dike-like units from Pitawala (2019). Associated uncertainties are within the size of the symbol. (Color online.)
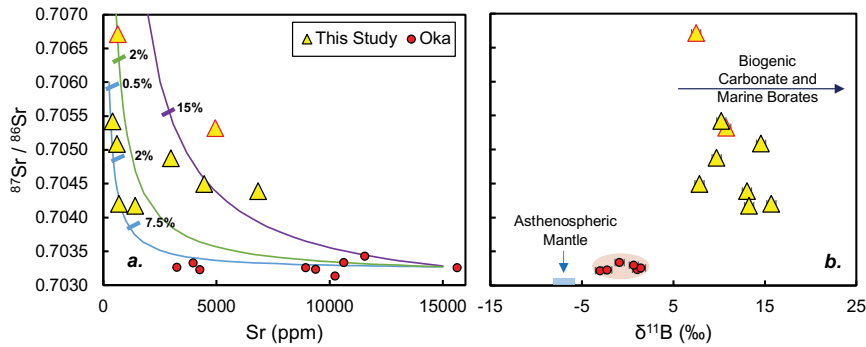
FIGURE 8. Sr isotopic compositions of samples of marble from the Grenville Province compared to (**a**) Sr concentrations and (**b**) $\delta^{11}B$ (‰) values. The two samples from the Adirondacks are outlined in red. Data on the Oka carbonatite complex (OCC) are from Chen and Simonetti (2015). (**a**) Lines represent different binary mixing lines between OCC and other end-members (blue: 260 ppm Sr, $^{87}Sr/^{86}Sr = 0.706$; green: 320 ppm Sr, $^{87}Sr/^{86}Sr = 0.710$; purple: 300 ppm Sr, $^{87}Sr/^{86}Sr = 0.730$; see text for details). (**b**) Blue region indicates the boron isotopic composition of asthenospheric (MORB-like) mantle (Marschall et al. 2017) and the blue arrow indicates the range of $\delta^{11}B$ values reported for biogenic carbonate and marine borates (Vengosh et al. 1991; Sutton et al. 2018; Swihart et al. 1986). Associated uncertainties are within the size of the symbol if not visible. (Color online.)
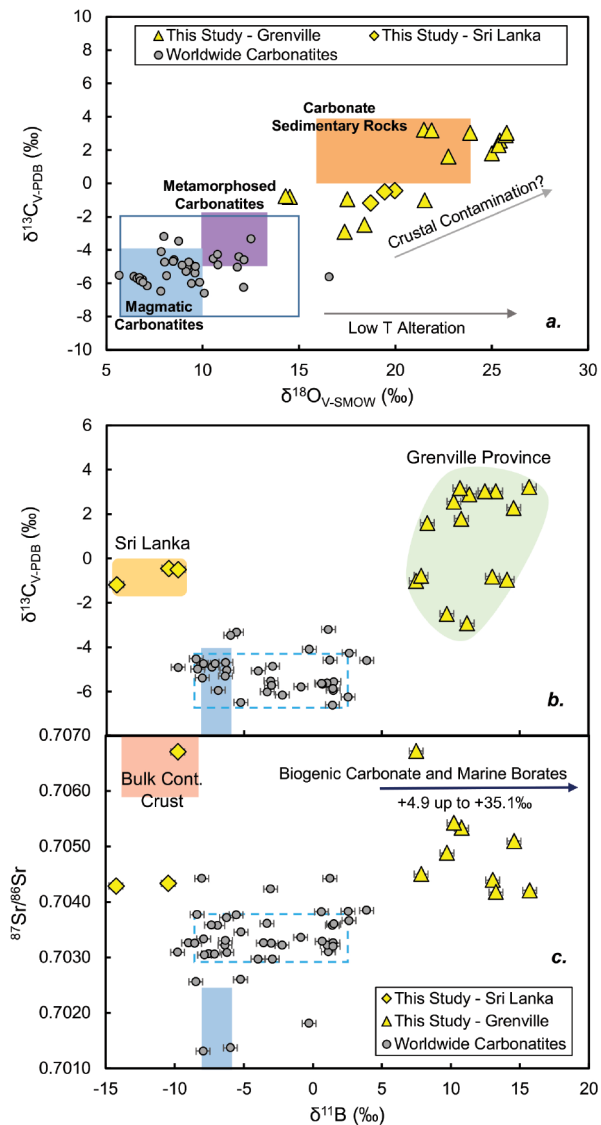
(Chen and Simonetti 2015; Hulett et al. 2016; Çimen et al. 2018, 2019; Kuebler et al. 2020). The Grenville Province samples are characterized by $\delta^{11}B$ values ranging between +7.5 and +15.7‰, which are similar to the values reported for sedimentary and biogenic carbonate (+4.9 to +35.1; Vengosh et al. 1991; Sutton et al. 2018). In contrast, the Sri Lanka carbonate samples are characterized by lighter $\delta^{11}B$ values (–9.8, –10.5, –14.3‰) than those for biogenic carbonate. The B isotope signatures for samples SL-07 and SL-10 overlap those estimated for the bulk continental crust (–9.4 ± 2.4‰; Marschall et al. 2017). Figure 9a compares the $\delta^{13}C_{V-PDB}$ and $\delta^{18}O_{V-SMOW}$ compositions for the samples studied to those for worldwide carbonatites; all of the data plot above and to the right relative to those for the carbonatite complexes. The $\delta^{13}C_{V-PDB}$ (Fig. 9b) and $^{87}Sr/^{86}Sr$ values (Fig. 9c) vs. $\delta^{11}B$ compositions for the marble samples and worldwide carbonatites are also shown, and these define three distinct fields corresponding to those from Sri Lanka, the Grenville Province, and worldwide

◀**FIGURE 9.** (**a**) $\delta^{13}C_{V-PDB}$ (‰) vs. $\delta^{18}O_{V-SMOW}$ (‰) values from this study (Grenville Province = yellow triangles; Sri Lanka = yellow diamonds) are compared to those for carbonatites worldwide (gray circles). (**a**) Fields for both magmatic (blue) and metamorphosed (purple) carbonatites along with carbonate sedimentary rocks (orange) are plotted (after Chiarenzelli et al. 2019); the blue line delineates the range of C and O isotope values that may be attributed to closed-system crystal fractionation of a single parental carbonatitic magma (Keller and Hoefs 1995). (**b**) $\delta^{13}C_{V-PDB}$ (‰) and (**c**) $^{87}Sr/^{86}Sr$ vs. $\delta^{11}B$ (‰) values for samples investigated in this study and those for carbonatites worldwide. Blue-shaded fields in **b** and **c** represent the boron isotopic composition of asthenospheric mantle (Marschall et al. 2017). The dashed blue box indicates the reported range of compositions for carbonatites worldwide deemed "pristine" on the basis of petrographic, radiogenic Sr, and C and O isotope compositions. The data for worldwide carbonatites are compiled from various sources (Chen and Simonetti 2015; Hulett et al. 2016; Çimen et al. 2018, 2019; Kuebler et al. 2020). (**c**) Average continental crust (red shaded box) estimated from Marschall et al. (2017) and Rudnick and Gao (2003). The range of $\delta^{11}B$ values reported for biogenic carbonate and marine borates is indicated with the arrow (Vengosh et al. 1991; Sutton et al. 2018; Swihart et al. 1986). The associated uncertainty is within the size of the symbol if not visible. (Color online.)

TABLE 3. Summary of leaching experiments on fragments of marble samples

	$\delta^{11}B$	Mass fraction of B (%)
SL-01 L	−10.9	0.14
SL-01 R	−16.1	0.86
SL-07 L	−16.3	0.19
SL-07 R	−18.2	0.81
SL-10 L	−17.0	0.17
SL-10 R	−14.9	0.83
BC-Cascade L	9.9	0.72
BC-Cascade R	6.7	0.28

Notes: L = leachate; R = residual-solid; $\delta^{11}B$ associated 2σ uncertainty (±0.5‰). Mass fraction values were calculated based on ICP-MS-determined B abundances and gravimetric measurements of the fragments before and after leaching.

TABLE 4. Strontium isotope data for select samples of marble from this study

	Rb (ppm)	Sr (ppm)	$^{87}Rb/^{86}Sr$	$^{87}Sr/^{86}Sr$	Uncertainty (2σ)
SL-01	0.01	146	0.00027	0.70428	0.00001
SL-07	0.03	1035	0.00010	0.70670	0.00002
SL-10	0.11	85	0.00371	0.70433	0.00001
BC-Harris	0.05	4942	0.00003	0.70533	0.00001
BC-Cascade	0.00	633	0.00001	0.70672	0.00001
WAK-02	0.06	2985	0.00006	0.70488	0.00001
BCJF	0.20	417	0.00143	0.70542	0.00001
GC-01	0.04	612	0.00018	0.70509	0.00001
YC-02	0.12	705	0.00052	0.70421	0.00001
OC-ST1	0.04	6842	0.00002	0.70439	0.00001
PC-01	0.29	4459	0.00020	0.70450	0.00001
JF	0.10	1416	0.00022	0.70417	0.00001

Notes: $^{87}Rb/^{86}Sr$ values were calculated based on ICP-MS-determined elemental abundances, which are associated with relative uncertainties of between 3 to 5% (2σ level).

samples of carbonatite. The results of the leaching experiments performed on several samples are listed in Table 3. For three of the four samples analyzed, the leachate has a heavier $\delta^{11}B$ value than the corresponding residue (SL-01, SL-07, BC-Cascade). In contrast, the leachate from sample SL-10 has a lighter $\delta^{11}B$ (−17.0‰) than its corresponding residue (−14.9‰).

Strontium isotope compositions

The strontium isotopic compositions of selected samples are listed in Table 4 and illustrated in Figures 8 and 9. The Sr contents range from 85 to 6842 ppm (Table 4) and are characterized by low-$^{87}Rb/^{86}Sr$ values (0.00001–0.0037). The reported $^{87}Sr/^{86}Sr$ values (0.70417–0.70672) are more radiogenic than the average $^{87}Sr/^{86}Sr$ (~0.70345) reported for carbonatites (Eppawala and Oka; Chen and Simonetti 2015) included for comparison in this study (Fig. 9c). The strontium isotopic values vs. their respective strontium concentrations and $\delta^{11}B$ values for the Grenville Province samples are compared to those for the Oka carbonatite complex in Figure 8 (Chen and Simonetti 2015). Figure 8a also exhibits several two-component binary mixing-model calculation lines between the Oka carbonatite (Sr abundance = 15 000 ppm and $^{87}Sr/^{86}Sr = 0.70327 \pm 0.00005$) and different end-members (blue: 260 ppm Sr, $^{87}Sr/^{86}Sr = 0.706$; 1.0–1.3 Ga seawater; Veizer 1989; green: 320 ppm Sr, $^{87}Sr/^{86}Sr = 0.710$; bulk continental crust; Rudnick and Gao 2003; Faure 1986; purple: 300 ppm Sr, $^{87}Sr/^{86}Sr = 0.730$; upper crust).

DISCUSSION

Origin of multi-colored marble

Grenville Province. As stated earlier, several models have been proposed for the origin of the multi-colored marbles from the Grenville Province, and these include (1) interaction of regional fluids released from surrounding metasediments, whether intrusion-related or not (Kitchen and Valley 1995; Bailey et al. 2019; Chiarenzelli et al. 2019); (2) metasomatism or melting of pre-existing carbonate deposit(s) via mantle-derived fluids (Moyd 1990; Lentz 1999; Sinaei-Esfahani 2013; Schumann and Martin 2016; Schumann et al. 2019); and (3) primary or metamorphosed carbonatite (Lumbers et al. 1990; Moecher et al. 1997). It is reasonable to expect that if the investigated samples are offshoots of primary carbonatites, then these would have mantle-like geochemical signatures since it is commonly accepted that carbonatites represent low-degree partial-melts of metasomatized upper mantle (Bell and Simonetti 2010). Some of these characteristics include REE enrichment (i.e.,

100–1000 ppm; Le Bas et al. 2002), magmatic stable isotope ratios ($\delta^{13}C_{V-PDB} \sim$ −4‰ to −8‰ and $\delta^{18}O_{V-SMOW} \sim$ +6‰ to +10‰; Keller and Hoefs 1995), depleted Sr signatures (<0.703; Bell and Simonetti 2010), and asthenospheric (MORB-like) B compositions (≤1 ppm; $\delta^{11}B \approx$ −7.1 ± 0.9‰; Hulett et al. 2016; Çimen et al. 2018, 2019; Kuebler et al. 2020). Based on the geochemical data reported here for the Grenville Province samples, these clearly have a metasedimentary rather than a mantle-derived origin. As Figure 6a illustrates, the REE contents for the Grenville Province samples are, in general, lower than those for typical calcio-carbonatites worldwide (Woolley and Kempe 1989) and the Meech Lake carbonatite (Hogarth 2016). The CN-REE patterns for the Grenville Province marble samples displayed in Figure 6a also differ from the steep, negatively sloped curves that are typical of carbonatites worldwide and are almost identical to the horizontal-like CN-REE pattern for the Otter Lake regional marble (dashed pink line; Figs. 6a and 6c). The elevated LREE concentrations, relative to the abundances reported for the regional marble, in most of the samples (except BC-ST4, BC-JF, and BC-Harris), may be attributed to micro-inclusions of REE-bearing apatite within the marble as documented in Sinaei-Esfahani (2013). This is consistent with the findings here that samples with the highest levels of mineral impurities (orange hues; Sinaei-Esfahani 2013), such as samples OC-ST3, OC-ST1, PC-01, have some of the highest LREE contents. In addition, the elevated HREE concentrations that characterize samples OC-ST1, OC-ST3, and PC-01 may be due to the presence of zircon (Chiarenzelli et al. 2019). In contrast, the BC-Cascade sample exhibits a negatively sloped CN-REE pattern that may be attributed to a compositional difference in the protolith.

The carbon and oxygen isotopic compositions for the Grenville Province samples listed in Table 2 and plotted in Figure 7a are also consistent with a sedimentary origin, as they plot above and to the right of both the magmatic and metamorphosed carbonatite fields (Keller and Hoefs 1995; Moecher et al. 1997). Moreover, the C and O isotope compositions for the Grenville Province samples are significantly heavier than carbonate from the Oka carbonatite, and plot mostly within the field for Lowlands marbles (green field in Fig. 7a; Kitchen and Valley 1995) and CMB skarn and marble (Lentz 1999). The wide range of $\delta^{13}C_{V-PDB}$ vs. $\delta^{18}O_{V-SMOW}$ values for samples of Lowland marble has been attributed to either an isotopically heterogeneous protolith (unmetamorphosed limestone) that underwent minor

isotopic exchange with inorganic carbon (graphite), which would decrease the original heavy isotopic signatures (e.g., $\delta^{13}C_{V\text{-PDB}}$ = 4‰, $\delta^{18}O_{V\text{-SMOW}}$ = 26‰; Peck et al. 2005; Chamberlain et al. 1999), or possible interaction with hydrothermal fluids during metamorphism (Valley and O'Neil 1984; Kretz 2001; Peck et al. 2005). Thus, the carbon and oxygen isotope signatures for the Grenville Province samples analyzed are most likely inherited from protolith limestone source(s) that experienced minor depletions in ^{18}O and ^{13}C due to fluid interaction associated with metamorphic activity.

The strontium abundances and isotope compositions for the samples of the Grenville Province marble (Table 4) further confirm their metasedimentary origin. The Sr concentrations for samples range from 238 to 6842 ppm, and though this range is highly variable, it is significantly lower than the average strontium abundance for the Oka carbonatite complex (~10 000 ppm; Chen and Simonetti 2015). Moreover, the $^{87}Sr/^{86}Sr$ values for the Grenville Province samples range between 0.70417 and 0.70542, which are more radiogenic than both the average $^{87}Sr/^{86}Sr$ value (~0.7034) for carbonatites included for comparison in this study (Fig. 9c) and the Oka carbonatite complex (0.70327; Chen and Simonetti 2015). Reported $^{87}Sr/^{86}Sr$ values for Grenville-age marbles (1.0–1.3 Ga) range from 0.7048 to 0.7050 (Krogh and Hurley 1968), which overlap the range of Sr isotope compositions for the marble samples studied here and confirm their biogenic origin. Note that sample BC-Cascade has a more radiogenic $^{87}Sr/^{86}Sr$ value (0.70672) compared to the remaining Grenville Province samples, an observation also described in Sinaei-Esfahani (2013), thus confirming the unique composition of its protolith.

Figure 8a also shows that the strontium isotopic compositions for a significant number of the Grenville Province samples plot along a two-component binary mixing line between an average 1.1–1.4 Ga seawater composition (260 ppm, $^{87}Sr/^{86}Sr$ = 0.706; Veizer 1989) and the Oka carbonatite complex (Chen and Simonetti 2015). The binary mixing calculations in Figure 8a indicate that only low contributions are required from a carbonatite end-member (between 0 to ~8%) to explain the Grenville Province marble samples data. Therefore, this effectively rules out any notion that these samples were derived via direct partial melting of a metasomatized upper mantle source. Figure 8a also displays additional two-component binary mixing curves based on both bulk continental crust and an upper crustal end-member (with varying and more radiogenic $^{87}Sr/^{86}Sr$ compositions), and none of these binary mixing calculations adequately explain the range of strontium compositions defined by the Grenville Province samples.

Although the geochemical data provide strong evidence for a metasedimentary origin for the Grenville Province samples, their corresponding boron contents and isotopic compositions greatly aid in the characterization of the fluids involved in their genesis. The boron concentrations (2.53 to 71.1 ppm; Table 1) for the Grenville Province marble samples are remarkably higher compared to those reported for carbonatites worldwide (≤1 ppm; Hulett et al. 2016; Çimen et al. 2018, 2019; Kuebler et al. 2020), and largely fall within the range reported for carbonate sediments and biogenic carbonates (0.3–54 ppm; Ishikawa and Nakamura 1993; Spivack and You 1997; Vengosh et al. 1991). Once again,

the sole exception is sample BC-Cascade, which has a much higher B concentration (71.1 ppm). One possible explanation is that the Adirondack Highlands region is characterized by a significant source of boron compared to both the Autoroute 5 and BC-Harris locations. For example, the limestone protolith(s) for BC-Cascade may have contained an evaporitic component that included borate minerals (characterized by wt% boron; Swihart et al. 1986), which is not uncommon in limestone deposited in a shallow marine setting (Smith and Holm 1990; Dickin and McNutt 2007; Chiarenzelli et al. 2015). This is consistent with studies by Grew et al. (1999) and Bailey et al. (2019) that reported the occurrence of numerous boron-bearing minerals (e.g., harkerite, datolite, tourmaline super group) within or adjacent to carbonate-rich metasedimentary units with evaporitic affinities in the Adirondacks region (including the Cascade Slide), and attributed the source of B to a calcareous protolith.

The boron isotopic compositions reported here (+7.5 to +15.7‰; Table 2) for the Grenville Province samples are similar to the highly variable and positive $\delta^{11}B$ values associated with biogenic carbonate and marine borates (from evaporite deposits). For example, foraminifera (calcite) are characterized by $\delta^{11}B$ values ranging from +4.9 to +32.2‰ (Vengosh et al. 1991), whereas marine borates (e.g., boracite, ulexite) have $\delta^{11}B$ values from +18.2 to +31.7‰ (Swihart et al. 1986). It is important to note that boron exhibits limited isotopic fractionation in carbonates under high-temperature (~450–750 °C) metamorphism (e.g., Çimen et al. 2019; Kuebler et al. 2020), much like the peak metamorphic conditions reported for the Grenville Province (Valley and O'Neil 1984; Kretz 2001). For example, Çimen et al. (2019) reported mantle-like $\delta^{11}B$ signatures (−8.67 to −6.36‰) for primary igneous carbonatites from the Blue River Region, British Columbia that underwent mid-amphibolite grade metamorphism. Thus, it is unlikely that these Grenville Province marble samples represent either primary or metamorphosed carbonatites or even marble metasomatized by "hot" mantle-derived fluids as their $\delta^{11}B$ values are much heavier than those reported for both carbonatites worldwide (Figs. 9b and 9c) and asthenospheric (MORB-like) mantle (−7.1 ± 0.9‰; Marschall et al. 2017). Hence, the B isotope compositions for the samples investigated here most likely reflect their sedimentary protolith, which is consistent with the REE abundances and $\delta^{13}C_{V\text{-PDB}}$ vs. $\delta^{18}O_{V\text{-SMOW}}$ values.

All of the combined geochemical data, in particular the boron isotope compositions presented here, support the hypothesis that these colored deposits formed from heterogeneous marine limestone units that may have interacted (slightly if at all) with regional fluids derived from surrounding metasediments (Kitchen and Valley 1995; Bailey et al. 2019; Chiarenzelli et al. 2019). The degree of interaction with additional crustal-derived fluids depends on the exact location of each sample. Several of the samples (BC-ST4, BC-JF, BC-Harris) closely match the characteristics (REE contents, CN-REE pattern, C and O stable isotopic ratios) of regional marble units. Thus, these carbonate deposits, in particular, likely represent typical units of metasedimentary marble within the Grenville Province and Adirondack Lowlands. However, the majority of the samples obtained from colored marble outcrops along Autoroute 5 (southwestern Québec) require an additional component to account for their REE enrichment and presence of significant mineral inclusions. One

possibility is that high-temperature hydrothermal fluids derived during the emplacement of proximal alkaline complexes of Oka and Meech Lake interacted with pelitic sediments and may have provided the elements (i.e., Fe, Si, LREE) necessary to precipitate the documented micro-inclusions (e.g., apatite, allanite, and diopside) in the marble samples; however, these would have to be B-poor, as their heavy $\delta^{11}B$ values are clearly inherited from their Precambrian marine carbonate protolith. Last, sample BC-Cascade is characterized by the most radiogenic $^{87}Sr/^{86}Sr$ ratio, which most likely reflects a slightly higher degree of fluid interaction with proximal metasedimentary units found within the Adirondack Highlands (Ashwal and Wooden 1983).

Sri Lanka. The multi-colored carbonate-rich dikes found in southwestern Sri Lanka have similarly been attributed to either an igneous, sedimentary, or mixed origin. Recently, Pitawala (2019) proposed that heat from shearing and thrusting between the HC and VC in Sri Lanka, associated with the suturing of Gondwana, melted marine carbonates and produced the dikes. The trace element abundances, C, O, B, and Sr isotopic data reported in this study, and outlined below, support this interpretation of a metasedimentary origin, but provide more insight into the nature of the fluids involved in their formation. The CN-REE plot (Fig. 6b) indicates that the Sri Lankan samples can be separated into two groups based on their color. The samples of blue marble (SL-01 and SL-10) have lower total REE abundances than both the average worldwide calcio-carbonatite (Woolley and Kempe 1989) and Eppawala carbonatite (Manthilake et al. 2008; Pitawala et al. 2003), which alone suggests a sedimentary origin, as limestone and marble are known to be depleted in REEs compared to carbonatites (Jarvis et al. 1975; Barker 1989; Subbarao et al. 1995; Le Bas et al. 2002). Furthermore, the CN-REE patterns for the blue samples do not overlap with either carbonatite profiles, and instead more closely resemble the horizontal-like pattern of the Sri Lankan regional marble field (Pitawala 2019). In contrast, the yellow sample (SL-07) has LREE contents that overlap with the carbonatite dike range, except for its La abundance (200 ppm; Table 1), which is similar to the La content of the Eppawala carbonatite (Manthilake et al. 2008; Pitawala et al. 2003). The mid-to-heavy-REE contents of sample SL-07 are intermediate between the values reported for carbonatite dikes and marbles (Pitawala 2019). The CN-REE pattern for sample SL-07 also displays similarities with both the Eppawala carbonatite and the carbonatite dikes, which is indicative of a mixed input.

The carbon and oxygen isotopic compositions for the Sri Lanka samples (Table 2), shown in Figure 7b, confirm their sedimentary origin as they plot above and to the right of both magmatic and metamorphosed carbonatite fields (Keller and Hoefs 1995; Moecher et al. 1997). The C and O isotope compositions for the investigated marble samples lie in-between values for nearby metasedimentary units and the Eppawala carbonatite and are entirely within the field previously defined for the dikes (Manthilake et al. 2008; Pitawala et al. 2003; Pitawala 2019). Notably, the Eppawala carbonatite is uniquely characterized by heavier C and O stable isotope signatures (relative to the magmatic carbonatite field), a feature that was attributed to an enriched mantle source region (Manthilake et al. 2008).

The reported Sr contents and isotope compositions for

samples of Sri Lankan marble are also consistent with a sedimentary origin (Table 4). Typically, carbonatites have significantly higher strontium contents (~7000 ppm) relative to sedimentary carbonates (260 ppm; Bell and Blenkinsop 1989); the same is true for the Eppawala carbonatite (2960–6819 ppm; Pitawala et al. 2003) compared to Sri Lankan regional marble units (~300 ppm; Pitawala et al. 2003). The Sr concentrations obtained for the samples analyzed in this study are on the same order as those for the regional marble; the samples of blue marble, however, have lower Sr abundances (85, 146 ppm; Table 4), whereas the sample of yellow marble has a higher Sr content (1035 ppm). The $^{87}Sr/^{86}Sr$ values for the blue samples (SL-01 and SL-10; Table 4) record less radiogenic values (0.70428, 0.70433) compared to the range reported for the Eppawala carbonatite (0.7049–0.7051; Manthilake et al. 2008). This enriched strontium isotope range documented for the Eppawala carbonatite, relative to the average for carbonatites worldwide included in this study (~0.7034; Fig. 9c), has been previously attributed to the presence of an enriched lithospheric mantle beneath the Indian sub-continent (Simonetti et al. 1998; Manthilake et al. 2008). In contrast, the sample of yellow marble (SL-07) has a more radiogenic value (0.70670) than both the Eppawala carbonatite and samples of blue marble, which overlaps with the Sr isotope ratio for bulk continental crust (0.706; Rudnick and Gao 2003). The less radiogenic Sr isotope values for the blue marble samples compared to both the Eppawala carbonatite and bulk continental crust are suspect; together with their low-Sr contents, these features suggest that they result from Sr loss associated with either secondary alteration due to weathering or fluid activity, or derivation from an isotopically depleted sediment. The former interpretation is favored, as it is supported by both the documented extensive weathering of Sri Lanka carbonate bodies, and the evidence for significant fluid activity surrounding the Eppawala carbonatite (Pitawala et al. 2003; Manthilake et al. 2008).

To evaluate the nature of the fluid(s) that formed the metasedimentary carbonate-rich dike occurrences in Sri Lanka, boron abundances and isotopic compositions are reported in Tables 3 and 4. The boron concentrations of the Sri Lanka samples in this study ranged from 1.48 to 2.44 ppm (Table 1) and are higher than the concentrations reported for a vast majority of carbonatites worldwide (≤1 ppm; Hulett et al. 2016). However, they are markedly lower than the boron content for biogenic carbonates (e.g., foraminifera, 9–54 ppm; Vengosh et al. 1991); and are not as variable as those reported for the Grenville Province samples (2.53 to 71.1 ppm; Table 1). The $\delta^{11}B$ values obtained for the Sri Lanka samples of multi-colored marble (–9.8 to –14.3‰) are depleted compared to both documented values for carbonatites worldwide (Figs. 9b and c) and biogenic carbonates (+4.9 to +35.1; Vengosh et al. 1991; Sutton et al. 2018), and align more closely with the range documented for bulk continental crust (–9.1 ± 2.4‰; Marschall et al. 2017). This value for bulk continental crust is based on studies of tourmaline in granitic bodies (Chaussidon and Albarède 1992; Marschall and Ludwig 2006) and is therefore biased toward metasedimentary sources. This may, in turn, be more representative of the influence of weathering (i.e., meteoric water) on stripping the heavier isotope (^{11}B) rather than reflecting the true composition of the continental crust. Analogously, the light $\delta^{11}B$ values for colored marble

samples from Sri Lanka, especially the blue samples, may reflect interaction with meteoric water rather than an inherited signature from a protolith. Furthermore, extensive weathering has been documented for the Eppawala carbonatite complex (and surrounding areas), which produced economic phosphate deposits (Pitawala et al. 2003). To investigate this hypothesis of possible preferential removal of ^{11}B via weathering, leaching experiments were performed on fragments of several samples under mildly acidic conditions (2% HNO_3); these tests yielded heavier $\delta^{11}B$ values in the leachates compared to residual solid fragments in three of the four samples investigated (e.g., –10.9‰ vs. –16.1‰; SL-01L-leachate vs. SL-01R-residue; Table 3). However, the leaching results listed in Table 3 also show that the effects of post-solidification alteration processes are not straightforward and may not always dictate the final $\delta^{11}B$ signature, as the leachate for sample SL-10 yielded a slightly lighter $\delta^{11}B$ value (–17.0‰) compared to its corresponding residue (–14.9‰).

The geochemical data, and in particular the boron isotope compositions obtained here, point to the formation of the carbonate-rich dikes in southwest Sri Lanka from fluids derived from the continental crust. It is unlikely that these deposits represent melted marine carbonates as proposed in Pitawala (2019), as their extremely light boron isotopic compositions do not corroborate this hypothesis. An alternative model possibly involves the interaction of low-temperature meteoric water with nearby marble deposits leading to carbonate- and ^{10}B-rich fluids concentrating and forming these multi-colored calcite-dominated dikes.

Boron isotope compositions: Effective tool in forensic studies

To demonstrate the effective use of boron isotope compositions in determining the petrogenesis of carbonate-rich rocks, Figure 9 compares the B isotope signatures for the marble samples investigated here to those reported to date for magmatic and pristine carbonates (mantle-derived carbonatites) worldwide. The data compiled for the carbonatite field relate only to pristine carbonates within the carbonatite samples (Hulett et al. 2016; Çimen et al. 2018, 2019; Kuebler et al. 2020). In Figure 9a, it is clear that the samples analyzed in this study are consistent with derivation from sedimentary source(s), as indicated by their enriched carbon and oxygen isotope signatures relative to both magmatic or metamorphosed carbonatite fields, and adjacent Rayleigh crystal fractionation field (Keller and Hoefs 1995; Moecher et al. 1997). However, $\delta^{13}C_{V-PDB}$ and $\delta^{18}O_{V-SMOW}$ compositions alone are not enough to distinguish between the Sri Lanka marbles and those from the Grenville Province (Fig. 9a). In addition, the assumption that crustal contamination has been recorded in magmatic carbonates based solely on heavy $\delta^{13}C_{V-PDB}$ and $\delta^{18}O_{V-SMOW}$ signatures is somewhat inadequate, especially in dolomite-dominated and geochemically complex magmatic-hydrothermal systems (e.g., Bayan Obo carbonatite complex; Chen et al. 2020; Kuebler et al. 2020).

First, the combined use of boron isotope compositions with corresponding $\delta^{13}C_{V-PDB}$ and $^{87}Sr/^{86}Sr$ ratios yields a clear distinction between the Sri Lanka and Grenville Province samples (Figs. 9b and 9c). The Sri Lanka samples are characterized by enriched $\delta^{13}C_{V-PDB}$, radiogenic $^{87}Sr/^{86}Sr$, and depleted $\delta^{11}B$ values compared to worldwide carbonatites, whereas the Grenville Province samples record enriched $\delta^{13}C_{V-PDB}$, $^{87}Sr/^{86}Sr$, and $\delta^{11}B$ values. The application of boron isotope ratios to these two groups of sedimentary carbonate-rich units allows them to be distinguished not only from each other but also identifies two potential modes of formation. The Grenville Province samples represent metamorphosed marine carbonates, whereas the Sri Lanka samples formed with input from crustal fluids. Thus, the results from this study indicate that boron isotope compositions can effectively identify sedimentary carbonate provenance.

Second, it is evident that boron isotope compositions are effective in distinguishing between mantle-derived and sedimentary carbonates when combined with both carbon and strontium isotope signatures. Despite the range of $\delta^{11}B$ values (~10‰) for carbonatites worldwide, B isotope signatures for mantle-derived carbonates are clearly distinct relative to those for sedimentary carbonates (Figs. 9b and c). Although the dashed box outlining the isotopic compositions for carbonatites worldwide covers a range of $\delta^{13}C_{V-PDB}$, $^{87}Sr/^{86}Sr$, and $\delta^{11}B$ values (Fig. 9), it does not come close to overlapping with either provenance field for the multi-colored marbles. Thus, the notion that heavy boron isotopic signatures in mantle-derived carbonates (i.e., > –7.1 ± 0.9‰) may be attributed solely to crustal contamination during magma emplacement, from either bulk continental crust or metasediments, is doubtful. The results from this study support the model proposed by Hulett et al. (2016) that the enriched boron isotopic compositions for young (<200 million years old) carbonatites reflect recycling of crustal material into their mantle source region rather than late-stage crustal contamination or hydrothermal alteration experienced during magma emplacement.

IMPLICATIONS

Comparison of the results for samples of multi-colored marble reported here with those for mantle-derived carbonates validates the use of boron (abundances) and its isotopes to distinguish between crustal and mantle-derived carbonates. The combined $\delta^{11}B$ values and $\delta^{13}C_{V-PDB}$ and $^{87}Sr/^{86}Sr$ compositions for mantle-derived carbonatites (e.g., Hulett et al. 2016; Çimen et al. 2018, 2019; Kuebler et al. 2020) are distinct from samples of marble from both regions investigated here. Grenville Province samples were derived from heterogeneous limestone protolith(s) that possibly contains an evaporite component, whereas Sri Lanka samples formed in carbonate-rich and ^{11}B-poor veins resulting from meteoric water interaction with crustal material. Based on the results reported here, it is clear that the low boron abundances (<<1 ppm) and relatively restricted range (about –8 to about +3‰) of boron isotopic compositions for worldwide mantle-derived carbonates cannot be readily explained by contamination with biogenic carbonate or meteoric water interaction during magma emplacement. Thus, the range of $\delta^{11}B$ values for carbonatites worldwide characterized by pristine radiogenic (Sr, Nd, and Pb) and magmatic-like $\delta^{13}C_{V-PDB}$ and $\delta^{18}O_{V-SMOW}$ isotope compositions reported to date (Hulett et al. 2016; Çimen et al. 2018, 2019; Kuebler et al. 2020) can conclusively be attributed to mantle source region heterogeneity.

References cited

Adams, F.D., and Barlow, A.E. (1910) Geology of the Haliburton and Bancroft areas, Ontario. Ontario Geological Survey, Memoir 6.

Ashwal, L.D., and Wooden, J.L. (1983) Sr and Nd isotope geochronology, geologic history, and origin of the Adirondack anothosite. Geochimica et Cosmochimica Acta, 47, 1875–1885.

Bailey, D.G., Lupulescu, M.V., Darling, R.S., Singer, J.W., and Chamberlain, S.C. (2019) A review of boron-bearing minerals (excluding tourmaline) in the Adirondack region of New York State. Minerals, 9, 644.

Baillieul, T.A. (1976) The Cascade Slide: A mineralogical investigation of a calc-silicate body on Cascade Mountain, Town of Keene, Essex County, New York. Master's thesis, University of Massachusetts at Amherst.

Balan, E., Pietrucci, F., Gervais, C., Blanchard, M., Schott, J., and Gaillardet, J. (2016) First-principles study of boron speciation in calcite and aragonite. Geochimica et Cosmochimica Acta, 193, 119–131.

Balboni, E., Jones, N., Spano, T., Simonetti, A., and Burns, P.C. (2016) Chemical and Sr isotopic characterization of North America uranium ores: Nuclear forensic applications. Applied Geochemistry, 74, 24–32.

Barker, D.S. (1989) Field relations of carbonatites. In K. Bell, Ed., Carbonatites: Genesis and Evolution, p. 38–69. Unwin Hyman, Boston, Massachusetts.

Basu, A.R., and Premo, W.R. (2001) U-Pb age of the Diana Complex and Adiron-dack granulite petrogenesis. Journal of Earth System Science, 110, 385–395.

Béland, R. (1955) Wakefield area, Gatineau County. Québec Ministère des Res-sources naturelles et de la Faune, DP 461.

Bell, K., and Blenkinsop, J. (1989) Neodymium and strontium isotope geochem-istry of carbonatites. In K. Bell, Ed., Carbonatites: Genesis and Evolution, p. 278–300. Unwin Hyman, Boston, Massachusetts.

Bell, K., and Simonetti, A. (2010) Source of parental melts to carbonatites—critical isotopic constraints. Mineralogy and Petrology, 98, 77–89.

Belley, P.M., Grice, J.G., Fayek, M., Kowalski, P.M., and Grew, E.S. (2014) A new occurrence of the borosilicate serendibite in tourmaline-bearing calc-silicate rocks, Portage-du-Fort Marble, Grenville Province, Québec: Evolution of boron isotope and tourmaline compositions in a metamorphic context. Canadian Mineralogist, 52, 595–616.

Belley, P.M., Picard, M., Rowe, R., and Poirier, G. (2016) Selected finds from the Highway 5 Extension: Wakefield Area, Outaouais, Québec, Canada. Rocks & Minerals, 91, 558–569.

Branson, O. (2018) Boron incorporation into marine $CaCO_3$. In H. Marschall and G. Foster, Eds., Boron Isotopes—The Fifth Element, p. 71–105. Springer.

Cartwright, I., and Weaver, T.R. (1993) Fluid-rock interaction between syenites and marbles at Stephen Cross Quarry, Québec, Canada: Petrological and stable isotope data. Contributions to Mineralogy and Petrology, 113, 533–544.

Chamberlain, S.C., King, V.T., Cooke, D., Robinson, G.W., and Holt, W. (1999) Minerals of the Gouverneur Talc Company Quarry (Valentine Deposit), Town of Diana, Lewis County, New York. Rocks & Minerals, 74, 236–249.

Chaussidon, M., and Albarède, F. (1992) Secular boron isotope variations in the continental crust: An ion microprobe study. Earth and Planetary Science Let-ters, 108, 229–241.

Chen, W., and Simonetti, A. (2013) In-situ determination of major and trace ele-ments in calcite and apatite, and U-Pb ages of apatite from the Oka carbonatite complex: Insights into a complex crystallization history. Chemical Geology, 353, 151–172.

——— (2015) Isotopic (Pb, Sr, Nd, C, O) evidence for plume-related sampling of an ancient, depleted mantle reservoir. Lithos, 216-217, 81–92.

Chen, W., Liu, H.-Y., Lu, J., Jiang, S.-Y., Simonetti, A., Xu, C., and Wen, Z. (2020) The formation of the ore-bearing dolomite marble from the giant Bayan Obo REE-Nb-Fe deposit, Inner Mongolia: Insights from micron-scale geochemical data. Mineralium Deposita, 55, 131–146.

Chiarenzelli, J., and Selleck, B. (2016) Bedrock geology of the Adirondack Region. Adirondack Journal of Environmental Studies, 221, 19–42.

Chiarenzelli, J., Kratzmann, D., Selleck, B., and de Lorraine, W. (2015) Age and provenance of Grenville supergroup rocks, Trans-Adirondack Basin, con-strained by detrital zircons. Geology, 43, 183–186.

Chiarenzelli, J.R., Lupulescu, M.V., Regan, S.P., and Singer, J.W. (2018) Age and origin of the Mesoproterozoic iron oxide-apatite mineralization, Cheever Mine, Eastern Adirondacks, NY. Geosciences, 8, 345.

Chiarenzelli, J., Lupulescu, M., Robinson, G., Bailey, D., and Singer, J. (2019) Age and origin of silicocarbonate pegmatites of the Adirondack region. Minerals, 9, 508.

Çimen, O., Kuebler, C., Monaco, B., Simonetti, S.S., Corcoran, L., Chen, W., and Simonetti, A. (2018) Boron, carbon, oxygen and radiogenic isotope investiga-tion of carbonatite from the Miaoya complex, central China: Evidences for late-stage REE hydrothermal event and mantle source heterogeneity. Lithos, 322, 225–237.

Çimen, O., Kuebler, C., Simonetti, S.S., Corcoran, L., Mitchell, R., and Simonetti,

A. (2019) Combined boron, radiogenic (Nd, Pb, Sr), stable (C, O) isotopic and geochemical investigations of carbonatites from the Blue River region, British Columbia (Canada): Implications for mantle sources and recycling of crustal carbon. Chemical Geology, 529, 119240.

Cooray, P.G. (1984) An Introduction to the Geology of Sri Lanka (Ceylon) 2nd ed., pp. 81–104 and 183–188. National Museum, Colombo, Sri Lanka.

——— (1994) The Precambrian of Sri Lanka: A historical review. Precambrian Research, 66, 3–18.

Coplen, T.B. (1995) Letter to the Editor: New IUPAC guidelines for the reporting of stable hydrogen, carbon, and oxygen isotope-ratio data. Journal of Research of the National Institute of Standards and Technology, 100, 285.

Coplen, T.B., Kendall, C., and Hopple, J. (1983) Comparison of stable isotope reference samples. Nature, 302, 236–238.

Corriveau, L. (2013) Structure of the Central Metasedimentary Belt in Québec, Grenville Province: An example from the analysis of high-grade metamorphic terranes. Geological Survey of Canada Bulletin 586 (in French).

Craig, H. (1957) Isotopic standards for carbon and oxygen and correction factors for mass-spectrometric analysis of carbon dioxide. Geochimica et Cosmochimica Acta, 12, 133–149.

De Hoog, J.C.M., and Savov, I.P. (2018) Boron isotopes as a tracer of subduc-tion zone processes. In H. Marschall and G. Foster, Eds., Boron Isotopes, p. 217–247. Springer.

Deegan, F.M., Troll, V.R., Whitehouse, M.J., Jolis, E.M., and Freda, C. (2016) Boron isotope fractionation in magma via crustal carbonate dissolution. Nature: Scientific Reports, 6, 30774.

Deines, P. (1989) Stable isotope variations. In K. Bell, Ed., Carbonatites: Genesis and Evolution, p. 300–359. Unwin Hyman, Boston, Massachusetts.

Dickin, A.P., and McNutt, R.H. (2007) The Central Metasedimentary Belt (Gren-ville Province) as a failed back-arc rift zone: Nd isotope evidence. Earth and Planetary Science Letters, 259, 97–106.

Faure, G. (1986) Principles of Isotope Geology. Wiley.

Fernando, G.W.A.R., Dharmapriya, P.L., and Baumgartner, L.P. (2017) Silica-undersaturated reaction zones at a crust-mantle interface in the Highland Com-plex, Sri Lanka: Mass transfer and melt infiltration during high-temperature metasomatism. Lithos, 284-285, 237–256.

Foster, G.L., Lécuyer, C., and Marschall, H.R. (2016) Boron stable isotopes. In W.M. White, Ed., Encyclopedia of Geochemistry, Encyclopedia Earth Science Series,1–6. Springer.

Gaillardet, J., and Lemarchand, D. (2018) Boron in the weathering environment. In H. Marschall and G. Foster, Eds., Boron Isotopes, p.163–188. Springer.

Gerdes, M.L., and Valley, J.W. (1994) Fluid flow and mass transport at the Valen-tine wollastonite deposit, Adirondack Mountains, New York State. Journal of Metamorphic Geology, 12, 589–608.

Gittins, J., Hayatsu, A., and York, D. (1970) A strontium isotope study of meta-morphosed limestones. Lithos, 3, 51–58.

Grew, E.S., Yates, M.G., and deLorraine, W. (1990) Serendibite from the northwest Adirondack Lowlands, in Russell, New York, U.S.A. Mineralogical Magazine, 54, 133–136.

Grew, E.S., Yates, M.G., Swihart, G.H., Moore, P.B., and Marquez, N. (1991) The paragenesis of serendibite at Johnsburg, New York, U.S.A.: An example of boron enrichment in the granulite facies. In L.L. Perchuk, Ed., Progress in Metamorphic and Magmatic Petrology, p. 247–285. Cambridge.

Grew, E.S., Yates, M.G., Adams, P., Kirkby, R., and Wiedenbeck, M. (1999) Harkerite and associated minerals in marble and skarn from the Crestmore Quarry, Riverside County, California and Cascade Slide, Adirondack Moun-tains, New York. Canadian Mineralogist, 37, 277–296.

He, X.-F., Santosh, M., Tsunogae, T., Malaviarachchi, S.P.K., and Dharmapriya, P.L. (2016) Neoproterozoic arc accretion along the 'eastern suture' in Sri Lanka during Gondwana assembly. Precambrian Research, 279, 57–80.

Hemming, N.G., and Hanson, G.N. (1992) Boron isotopic composition and concentration in modern marine carbonates. Geochimica et Cosmochimica Acta, 56, 537–543.

Hemming, N.G., Reeder, R.J., and Hanson, G.N. (1995) Mineral-fluid partitioning and isotopic fractionation of boron in synthetic calcium carbonate. Geochimica et Cosmochimica Acta, 59, 371–379.

Hewitt, D.F. (1967) Uranium and thorium deposits of southern Ontario. Ontario Department of Mines, Mineral Resources Circular 4.

Hogarth, D.D. (1989) Pyrochlore, apatite and amphibole: distinctive minerals in carbonatite. In K. Bell, Ed., Carbonatites: Genesis and Evolution, p.105–148. Unwin Hyman, Boston, Massachusetts.

——— (2016) Chemical trends in the Meech Lake, Québec, carbonatites and fenites. Canadian Mineralogist, 54, 1105–1128.

Hulett, S.R.W., Simonetti, A., Rasbury, E.T., and Hemming, N.G. (2016) Recycling of subducted crustal components into carbonatite melts revealed by boron isotopes. Nature Geoscience, 9, 904–909.

Ishikawa, T., and Nakamura, E. (1993) Boron isotope systematics of marine sedi-ments. Earth and Planetary Science Letters, 117, 567–580.

Jarvis, J.C., Wildeman, T.R., and Banks, N.G. (1975) Rare earths in the Leadville limestone and its marble derivatives. Chemical Geology, 16, 27–37.

Jenner, G.A., Longerich, H.P., Jackson, S.E., and Fryer, B.J. (1990) ICP-MS—A powerful tool for high-precision trace element analysis in Earth sciences: Evidence from analysis of selected U.S.G.S. reference samples. Chemical Geology, 83, 133–148.

Keller, J., and Hoefs, J. (1995) Stable isotope characteristics of recent natrocarbonatites from Oldoinyo Lengai. In K. Bell and J. Keller, Eds., Carbonatite Volcanism, IAVCEI Proceedings in Volcanology, 4, p. 113–123. Springer.

Kitchen, N.E., and Valley, J. (1995) Carbon isotope thermometry in marbles of the Adirondack Mountains, New York. Journal of Metamorphic Geology, 13, 577–594.

Kowalski, P., and Wunder, B. (2018) Boron-isotope fractionation among solids-fluids-melts: experiments and atomic modeling. In H. Marschall and G. Foster, Eds., Boron Isotopes—The Fifth Element, vol. 7, Ch. 3, p. 33–69. Springer.

Kretz, R. (2001) Oxygen and carbon isotopic composition of Grenville marble, and an appraisal of equilibrium in the distribution of isotopes between calcite and associated minerals, Otter Lake area, Québec, Canada. Canadian Mineralogist, 39, 1455–1472.

Krogh, T.E., and Hurley, P.M. (1968) Strontium isotope variation and whole-rock isochron studies, Grenville Province of Ontario. Journal of Geophysical Research, 73, 7107–7125.

Kröner, A., Cooray, P.G., and Vitanage, P.W. (1991) Lithotectonic subdivisions of the Precambrian basement in Sri Lanka. In A. Kröner, Ed., Part 1. Summary of Research of the German-Sri Lankan Consortium, Geological Survey Department, Lefkosia, pp. 5–21.

Kröner, A., Kehelpannala, K.V.W., and Hegner, E. (2003) Ca. 700–1000 Ma magmatic events and Grenvillian-age deformation in Sri Lanka: Relevance for Rodinia supercontinent formation and dispersal, and Gondwana amalgamation. Journal of Asian Earth Sciences, 22, 279–300.

Kuebler, C., Simonetti, A., Chen, W., and Simonetti, S.S. (2020) Boron isotopic investigation of the Bayan Obo carbonatite complex: Insights into the source of mantle carbon and hydrothermal alteration. Chemical Geology, 557, 119859. https://doi.org/10.1016/j.chemgeo.2020.119859

Le Bas, M.J., Subbarao, K.V., and Walsh, J.N. (2002) Metacarbonatite or marble?—the case of the carbonate, pyroxenite, calcite-apatite rock complex at Borra, Eastern Ghats, India. Journal of Asian Earth Sciences, 20, 127–140.

Lemarchand, D., Gaillardet, J., Lewin, É., and Allègre, C.J. (2000) The influence of rivers on marine boron isotopes and implications for reconstructing past ocean pH. Nature, 408, 951–954.

——— (2002) Boron isotope systematics in large rivers: implications for the marine boron budget and paleo-pH reconstruction over the Cenozoic. Chemical Geology, 190, 123–140.

Lentz, D. (1996) U, Mo, and REE mineralization in late-tectonic granitic pegmatites, southwestern Grenville Province, Canada. Ore Geology Reviews, 11, 197–227.

——— (1999) Carbonatite genesis: A reexamination of the role of intrusion-related pneumatolytic skarn processes in limestone melting. Geology, 27, 335–338.

Lumbers, S.B., Heaman, L.M., Vertolli, V.M., and Wu, T.-W. (1990) Nature and timing of Middle Proterozoic magmatism in the Central Metasedimentary Belt, Grenville Province, Ontario. In C.F. Gower, T. Rivers, and B. Ryan, Eds., Mid-Proterozoic Laurentia-Baltica, Special Paper, 38, 243–278. Geological Association of Canada.

Madugalla, N.S., and Pitawala, A. (2015) Calcite deposits associated with marble in the Balangoda area, Sri Lanka. Recent Contribution to the Geology of Sri Lanka-Excursion Guide, 10, 25–29.

Madugalla, T.B.N.S., Pitawala, H.M.T.G.A., and Karunaratne, D.G.G.P. (2014) Use of carbonates in the production of precipitated calcium carbonate: A case study from Eppawala, Sri Lanka. Natural Resources Research, 23, 217–229.

Madugalla, N.S., Pitawala, A., and Manthilake, G. (2017) Primary and secondary textures of dolomite in Eppawala carbonatites, Sri Lanka: implications for their petrogenetic history. Journal of Geosciences, 62, 187–200.

Manthilake, M.A.G.M., Sawada, Y., and Sakai, S. (2008) Genesis and evolution of Eppawala carbonatites, Sri Lanka. Journal of Asian Earth Sciences, 32, 66–75.

Mantilaka, M.M.M.G.P.G., Karunaratne, D.G.G.P., Rajapakse, R.M.G., and Pitawala, H.M.T.G.A. (2013) Precipitated calcium carbonate/poly(methyl methacrylate) nanocomposite using dolomite: Synthesis, characterization and properties. Powder Technology, 235, 628–632.

Mantilaka, M.M.M.G.P.G., Rajapakse, R.M.G., Karunaratne, D.G.G.P., and Pitawala, H.M.T.G.A. (2014a) Preparation of amorphous calcium carbonate nanoparticles from impure dolomitic marble with the aid of poly (acrylic acid) as a stabilizer. Advanced Powder Technology, 25, 591–598.

Mantilaka, M.M.M.G.P.G., Wijesinghe, W.P.S.L., Rajapakse, R.M.G., Karunaratne, D.G.G.P., and Pitawala, H.M.T.G.A. (2014b) Surfactant assisted synthesis of pure calcium carbonate nanoparticles from Sri Lankan dolomite. Journal of the National Science Foundation, 43, 237–244.

Marschall, H.R., and Ludwig, T. (2006) Re-examination of the boron isotopic composition of tourmaline from the Lavicky granite, Czech Republic, by secondary ion mass spectrometry: back to normal. Critical comment on "Chemical and boron isotopic composition of tourmaline from the Lavicky leucogranite, Czech Republic" by S.-Y. Jiang et al., Geochemical Journal, 37, 545–556, 2003. Geochemical Journal, 40, 631–638.

Marschall, H.R., Wanless, V.D., Shimizu, N., Pogge von Strandmann, P.A.E., Elliott, T., and Monteleone, B.D. (2017) The boron and lithium isotopic composition of mid-ocean ridge basalts and the mantle. Geochimica et Cosmochimica Acta, 207, 102–138.

Matt, P., Powell, W., Volkert, R., Gorring, M., and Johnson, A. (2017) Sedimentary exhalative origin for magnetite deposits of the New Jersey Highlands. Canadian Journal of Earth Sciences, 54, 1008–1023.

McCrea, J.M. (1950) On the isotopic chemistry of carbonates and a paleotemperature scale. The Journal of Chemical Physics, 18, 849–857.

McLelland, J.M., Selleck, B.W., and Bickford, M.E. (2013) Tectonic evolution of the Adirondack Mountains and Grenville Orogen Inliers within the U.S.A. Geoscience Canada, 40, 318–352.

Milisenda, C.C., Liew, T.C., Hofmann, A.W., and Kröner, A. (1988) Isotopic mapping of age provinces in precambrian high-grade terrains: Sri Lanka. The Journal of Geology, 96, 608–615.

Milisenda, C.C., Liewa, T.C., Hofmanna, A.W., and Köhler, H. (1994) Nd isotopic mapping of the Sri Lanka basement: update and additional constraints from Sr isotopes. Precambrian Research, 66, 95–110.

Moecher, D.P., Anderson, E.D., Cook, C.A., and Mezger, K. (1997) The petrogenesis of metamorphosed carbonatites in the Grenville Province, Ontario. Canadian Journal of Earth Sciences, 34, 1185–1201.

Moyd, L. (1990) Davis Hill near Bancroft Ontario: An occurrence of large nepheline, biotite, albite-antiperthite crystals in calcite cored vein-dykes. The Mineralogical Record, 21, 235–245.

Osanai, Y., Ando, K.T., Miyashita, Y., Kusachi, I., Yamasaki, T., Doyama, D., Prame, W.K.B.N., Jayatilake, S., and Mathavan, V. (2000) Geological field work in the southwestern and central parts of the Highland complex, Sri Lanka during 1998–1999, special reference to the highest grade metamorphic rocks. Journal of Geoscience, Osaka City University, 43, 227–247.

Osanai, Y., Sajeev, K., Owada, M., Kehelpannala, K.V.W., Prame, W.K.B.N., Nakano, N., and Jayatileke, S. (2006) Metamorphic evolution of ultrahigh-temperature and high pressure granulites from Highland Complex, Sri Lanka. Journal of Asian Earth Sciences, 28, 20–37.

Palmer, M.R., and Swihart, G.H. (1996) Boron isotope geochemistry: An overview. In E.S.Grew and L.M. Anovitz, Eds., Boron: Mineralogy, Petrology, and Geochemistry, 33, p. 709–740. Reviews in Mineralogy and Geochemistry, Mineralogical Society of America, Chantilly, Virginia.

Peck, W.H., DeAngelis, M.T., Meredith, M.T., and Morin, E. (2005) Polymetamorphism of marbles in the Morin terrane, Grenville Province, Québec. Canadian Journal of Earth Sciences, 42, 1949–1965.

Penman, D.E., Hönisch, B., Rasbury, E.T., Hemming, N.G., and Spero, H.J. (2013) Boron, carbon, and oxygen isotopic composition of brachiopod shells: Intra-shell variability, controls, and potential as a paleo-pH recorder. Chemical Geology, 340, 32–39.

Pitawala, A. (2019) Mineralogy, petrology, geochemistry and economic potential of carbonate rocks of Sri Lanka. Journal of the Geological Society of Sri Lanka, 20, 1–13.

Pitawala, A., and Lottermoser, B.G. (2012) Petrogenesis of the Eppawala carbonatites, Sri Lanka: A cathodoluminescence and electron microprobe study. Mineralogy and Petrology, 105, 57–70.

Pitawala, A., Schidlowski, M., Dahanayake, K., and Hofmeister, W. (2003) Geochemical and petrological characteristics of Eppawala phosphate deposits. Mineralium Deposita, 38, 505–515.

Rae, J.W.B. (2018) Boron isotopes in foraminifera: systematics, biomineralisation, and CO₂ reconstruction. In H. Marschall and G. Foster, Eds., Boron Isotopes, p.107–143. Springer.

Rasbury, E.T., and Hemming, N.G. (2017) Boron isotopes: A "Paleo-pH Meter" for tracking ancient atmospheric CO₂. Elements, 13, 243–248.

Rudnick, R.L., and Gao, S. (2003) Composition of the Continental Crust. Treatise on Geochemistry, 3, 1–64.

Sanyal, A., Nugent, M., Reeder, R.J., and Bijma, J. (2000) Seawater pH control on the boron isotopic composition of calcite: evidence from inorganic calcite precipitation experiments. Geochimica et Cosmochimica Acta, 64, 1551–1555.

Satterly, J. (1956) Radioactive deposits in the Bancroft area. Ontario Department of Mines, Annual Report, Vol. 65, part 6.

Schumann, D., and Martin, R.F. (2016) Blue calcite in the Grenville Province: Evidence of melting (online). Available: https://gsa.confex.com/gsa/2016NE/webprogram/Paper272356.html. Abstracts with program, Geological Society of America Annual Meeting, March 2016.

Schumann, D., Martin, R.F., Fuchs, S., and de Fourestier, J. (2019) Silicocarbonatitic melt inclusions in fluorapatite from the Yates Prospect, Otter Lake, Quebec: Evidence of marble anatexis in the Central Metasedimentary Belt of the Grenville Province. Canadian Mineralogist, 57, 583–604.

Simonetti, A., Goldstein, S.L., Schmidberger, S.S., and Viladkar, S.G. (1998) Geochemical and Nd, Pb, and Sr isotope data from Deccan alkaline complexes-inferences for mantle sources and plume–lithosphere interaction. Journal of Petrology, 39, 1847–1864.

Sinaei-Esfahani, F. (2013) Localized metasomatism of Grenvillian marble leading to its melting, Autoroute 5 near Old Chelsea, Quebec. Master's thesis, McGill

University, Montreal.

Smith, T.E., and Holm, P.E. (1990) The geochemistry and tectonic significance of pre-metamorphic minor intrusions of the Central Metasedimentary Belt, Grenville Province, Canada. Precambrian Research, 48, 341–360.

Spivack, A.J., and Edmond, J.M. (1987) Boron isotope exchange between seawater and the oceanic crust. Geochimica et Cosmochimica Acta, 51, 1033–1043.

Spivack, A.J., and You, C.F. (1997) Boron isotopic geochemistry of carbonates and pore waters, Ocean Drilling Program Site 851. Earth and Planetary Science Letters, 152, 113–122.

Subbarao, K.V., Le Bas, M.J., and Bhaskar, R. (1995) Are the Vinjamur rocks carbonatites or meta-limestones? Journal of Geological Society of India, 46, 125–137.

Sun, S.-S., and McDonough, W.F. (1989) Chemical and isotopic systematics of oceanic basalts: implications for mantle composition and processes. In A.D. Saunders and M.J. Norry, Eds., Magmatism in Ocean Basins, 42, p. 313–345. Geological Society of London Special Publication, U.K.

Sutton, J.N., Liu, Y.-W., Ries, J.B., Guillermic, M., Ponzevera, E., and Eagle, R.A. (2018) $\delta^{11}B$ as monitor of calcification site pH in divergent marine calcifying organisms. Biogeosciences, 15, 1447–1467.

Swihart, G.H., Moore, P.B., and Callis, E.L. (1986) Boron isotopic composition of marine and nonmarine evaporite borates. Geochimica et Cosmochimica Acta, 50, 1297–1301.

Tollo, R.P., Bartholomew, M.J., Hibbard, J.P., and Karabinos, P.M. (2010) From Rodinia to Pangea: The Lithotectonic Record of the Appalachian Region. Geological Society of America Memoir, 206.

Valley, J.W., and O'Neil, J.R. (1984) Fluid heterogeneity during granulite facies metamorphism in the Adirondacks: Stable isotope evidence. Contributions to Mineralogy and Petrology, 85, 158–173.

Veizer, J. (1989) Strontium isotopes in seawater through time. Annual Review of Earth and Planetary Sciences, 17, 141–167.

Vengosh, A., Kolodny, Y., Starinsky, A., Chivas, A.R., and McCulloch, M.T. (1991) Coprecipitation and isotopic fractionation of boron in modern biogenic carbonates. Geochimica et Cosmochimica Acta, 55, 2901–2910.

Viladkar, S.G., and Subramanian, V. (1995) Mineralogy and geochemistry of the carbonatites of the Sevathur and Samalpatti complex, Tamil Nadu. Journal of the Geological Society of India, 45, 505–517.

Vistelius, A.B., Agterberg, F.P., Divi, S.R., and Hogarth, D.D. (1983) A stochastic model for the crystallization and textural analysis of a fine grained granitic stock near Meech Lake, Gatineau Park, Quebec. Geological Survey of Canada. https://doi.org/10.4095/109255.

Weerakoon, M.W.K., Miyazaki, T., Shuto, K., and Kagami, H. (2001) Rb-Sr and Sm-Nd geochronology of the Eppawala metamorphic rocks and carbonatite, Wanni Complex, Sri Lanka. Gondwana Research, 4, 409–420.

Woolley, A.R., and Kempe, D.R.C. (1989) Carbonatites: nomenclature, average chemical compositions, and element distribution. In K. Bell, Ed., Carbonatites: Genesis and Evolution, p.1–14. Unwin Hyman, Boston, Massachusetts.

Endnote:

[1]Deposit item AM-22-17811, Online Materials. Deposit items are free to all readers and found on the MSA website, via the specific issue's Table of Contents (go to http://www.minsocam.org/MSA/AmMin/TOC/2022/Jan2022_data/Jan2022_data.html).